The genetic diversity, morphology, biogeography, and taxonomic designations of Ammonia (Foraminifera) in the Northeast Atlantic

The genetic diversity, morphology, biogeography, and taxonomic designations of Ammonia (Foraminifera) in the Northeast Atlantic

Clare Bird, Magali Schweizer, Angela Roberts, William E.N. Austin, Karen Luise Knudsen, Katharine M. Evans, Helena L. Filipsson, Martin D.J. Sayer, Emmanuelle Geslin, Kate F. Darling

PII: S0377-8398(18)30086-0
DOI: https://doi.org/10.1016/j.marmicro.2019.02.001
Reference: MARMIC 1726

To appear in: *Marine Micropaleontology*

Received date: 6 July 2018
Revised date: 11 January 2019
Accepted date: 7 February 2019

Please cite this article as: C. Bird, M. Schweizer, A. Roberts, et al., The genetic diversity, morphology, biogeography, and taxonomic designations of Ammonia (Foraminifera) in the Northeast Atlantic, Marine Micropaleontology, https://doi.org/10.1016/j.marmicro.2019.02.001

The genetic diversity, morphology, biogeography, and taxonomic designations of *Ammonia* (Foraminifera) in the Northeast Atlantic

Clare Bird[a,1,*], Magali Schweizer[a,b], Angela Roberts[c], William E.N. Austin[c,d], Karen Luise Knudsen[e], Katharine M. Evans[a], Helena L. Filipsson[f], Martin D. J. Sayer[g], Emmanuelle Geslin[b], Kate F. Darling[a,c]

[a]School of Geosciences, University of Edinburgh, West Mains Road, Edinburgh, EH9 3JW, UK

[b]UMR CNRS 6112 LPG-BIAF, University of Angers, 2 Bd Lavoisier, 49045 Angers Cedex 1, France

[c]School of Geography and Sustainable Development, University of St Andrews, North Street, St Andrews KY16 9AL, UK

[d]Scottish Association for Marine Science, Scottish Marine Institute, Oban PA37, 1QA, U

[e]Department of Geoscience, Aarhus University, Høegh-Guldbergs Gade 2, DK-8000 Aarhus C, Denmark

[f]Department of Geology, Lund University, Sölvegatan 12, 223 62 Lund, Sweden

[g]NERC National Facility for Scientific Diving, Scottish Association for Marine Science, Dunbeg, Oban PA37 1QA, UK

*corresponding author: clare.bird2@stir.ac.uk

[1]current address: Biological and Environmental Sciences, Cottrell Building, University of Stirling, Stirling, FK9 4LA, UK.

Abstract

The genetic diversity, morphology and biogeography of *Ammonia* specimens was investigated across the Northeast (NE) Atlantic margins, to enhance the regional (palaeo)ecological studies based on this genus. Living specimens were collected from 22 sampling locations ranging from Shetland to Portugal to determine the distribution of *Ammonia* genetic types across the NE Atlantic shelf biomes. We successfully imaged (via scanning electron microscopy, SEM) and genotyped 378 *Ammonia* specimens, based on the small subunit (SSU) rRNA gene, linking morphology to genetic type. Phylogenetic analyses enabled identification of seven genetic types and subtypes inhabiting the NE Atlantic margins. Where possible, we linked SSU genetic types to the established large subunit (LSU) T-type nomenclature of Hayward et al. (2004). SSU genetic types with no matching T-type LSU gene sequences in GenBank were allocated new T-numbers to bring them in line with the widely adopted T-type nomenclature. The genetic types identified in the NE Atlantic margins

are T1, T2, T3, T6, and T15, with both T2 and T3 being split further into the subtypes T2A and T2B, and T3S and T3V respectively. The seven genetic types and subtypes exhibit different biogeographical distributions and/or ecological preferences, but co-occurrence of two or more genetic types is common. A shore-line transect at Dartmouth (South England) demonstrates that sampling position on shore (high, middle or low shore) influences the genetic type collected, the numbers of genetic types that co-occur, and the numbers of individuals collected. We performed morphometric analysis on the SEM images of 158 genotyped *Ammonia* specimens. T15 and the subtypes T3S and T3V can be morphologically distinguished. We can unequivocally assign the taxonomic names *A. batava* and *A. falsobeccarii* to T3S and T15, respectively. However, the end members of T1, T2A, T2B and T6 cannot be unambiguously distinguished, and therefore these genetic types are partially cryptic. However, we confirm that T2A can be assigned to *A. aberdoveyensis,* but caution must be taken in warm provinces where the presence of T2B will complicate the morphological identification of T2A. We suggest that T6 should not currently be allocated to the Pliocene species *A. aomoriensis* due to morphological discrepancies with the taxonomic description and to the lack of genetic information. Of significance is that these partially cryptic genetic types frequently co-occur, which has considerable implications for precise species identification and accurate data interpretation.

Keywords: *Ammonia;* genetic types; morphometrics; biogeography; taxonomy

1. Introduction

Ammonia is amongst the most abundant and diverse genera of benthic foraminifera worldwide, with possibly as many as 25-30 biological species (Hayward et al., 2004). They occur in the most marginal marine environments with >80% mud/silt, from salt marsh and estuaries to subtidal habitats. Although members of the group are able to cope with the broad range of salinities, oxygen levels and temperatures associated with these habitats, they appear absent from the colder high latitudes (Murray, 1991, 2006). Coastal margin benthic foraminifera, including *Ammonia*, are used in a variety of (palaeo)environmental studies such as monitoring pollution (e.g., Le Cadre and Debenay, 2006; Frontalini and Coccioni, 2008; 2011; Foster et al., 2012; Jorissen et al., 2018), determining sea level changes over time (e.g., Gehrels et al., 2005; Horton and Edwards 2006) and also as proxies in palaeoclimate reconstructions (e.g., Sejrup et al., 2004; Groeneveld and Filipsson, 2013; Dutton et al., 2015; Groeneveld et al., 2018). In addition, since *Ammonia* is easy to collect and culture, it is routinely used for laboratory experiments (e.g., de Nooijer et al., 2009; Keul et al., 2013; Toyofuku et al., 2017). Such studies require a sound understanding of the species concept,

since inaccuracy in determining species would result in invalid ecological and biogeographic data application. Further, modern palaeoproxy calibrations are often species-specific (e.g., Rosenthal et al., 1997; Elderfield et al., 2006; Healey et al., 2008), and it is therefore critical to establish and apply the species-specific calibrations to the correct species.

In foraminifera, taxonomists primarily utilise the morphological characteristics of the test to classify taxa and describe morphospecies (e.g., Loeblich and Tappan, 1987). Despite rigorous taxonomic descriptions and revisions (Ellis and Messina, 1940 and supplements), the inconsistent application of species names and associated synonyms (Boltovskoy and Wright, 1976; Haynes, 1992; Pawlowski and Holzmann, 2008) remains a major problem for studies using benthic foraminifera. This inconsistency is a cause of particular confusion between members of the genus *Ammonia*, as they exhibit high morphological variation. Whether this variation is a result of ecophenotypic traits or species differences has generated much debate (for a comprehensive review see Holzmann, 2000 and references therein) and highlights the problems of relying solely on morphological traits for species designation. However, by utilising a combination of molecular characterisation and morphological traits, it is possible to distinguish some of the morphological boundaries that separate the genetic types of *Ammonia*. Globally to date, genetic characterisation of the large sub-unit (LSU) rRNA gene, herein referred to as the LSU, has revealed 14 genetic types within *Ammonia*, that exhibit varying degrees of morphological distinction (Pawlowski et al., 1995; Holzmann and Pawlowski, 2000; Hayward et al., 2004; Toyofuku et al., 2005; Schweizer et al., 2011b; Saad and Wade, 2016). For practical application, the difficulty arises in linking these characterised genetic types to previously described *Ammonia* morphospecies. For *Ammonia*, Hayward et al. (2004) have undertaken the morphological comparison between genetically characterised specimens using the LSU and type material. These authors identified 13 *Ammonia* genetic types, designated T1-T13, of which eight were considered to have been described already, and the associated taxonomic names were therefore assigned to them.

The T-type nomenclature for *Ammonia* is now well established in the literature. For example, a number of studies have utilised the type descriptions and genetic T-type nomenclature of Hayward et al. (2004), to give taxonomic names to morphologically described (Dissard et al., 2010; Nehrke et al., 2013) and to genetically characterised (Schweizer et al., 2011b; Lei et al., 2016) *Ammonia* specimens. However, many contemporary studies still rely on using morphological taxonomic assignments without reference to the taxonomic descriptions supported by molecular evidence as proposed by Darling et al. (2016) and Roberts et al. (2016). Morphological traits used for species distinction can prove erroneous following genetic characterisation and true ecophenotypic morphological characters could remain

unrecognised. Incorrect taxonomic assignments in the literature leads to the merging of mismatched data and flawed interpretation and conclusions. These issues demand that a more rigorous taxonomy should be used for *Ammonia*, based on molecular characterisation and morphometric analysis together with a morphological description of the SEM images associated with each individual genetic type (Darling et al, 2016). If genetic types are found to possess differentiating morphological characters, this should be followed by the allocation of the most appropriate taxonomic name by comparison with formal type descriptions. Ideally, morphospecies names should not therefore be placed onto molecular phylogenies, unless both the morphology and genetic type have been linked to a formally named holotype (e.g., Darling et al., 2016; Roberts et al., 2016). Once established, the rigorous taxonomic link provides a better understanding of the true biogeography and co-occurrences of genetic types that can be morphologically discriminated from those that remain cryptic, and of the ecological niches that they occupy.

While the genetic characterisation of *Ammonia* specimens using the LSU enabled the development of the genetic type nomenclature for *Ammonia* (T-type; Hayward et al., 2004), it is not the principle gene used for the study of molecular diversity and genetic characterisation in microorganisms, which includes the foraminifera. Instead, the small sub-unit (SSU) rRNA gene, herein called the SSU, is the most commonly used marker. For example, curated databases developed for linking DNA to morphologically based taxonomies in eukaryotes, such as the SILVA rRNA database (Quast et al., 2013), the Protist Ribosomal Reference Database (PR^2, Guillou et al., 2013) and the PFR^2 database for planktonic foraminifera (Morard et al., 2015), all use the SSU. SSU sequences allow the discrimination of most foraminiferal species (Pawlowski et al., 2012), and make up the majority of foraminiferal sequences deposited in publicly available databases such as GenBank (http://www.ncbi.nlm.nih.gov/genbank/).

The main reference databases for the benthic foraminifera are the forambarcoding database (http://forambarcoding.unige.ch/; Pawlowski and Holzmann, 2014) and the 37f database (Pawlowski and Lecroq, 2010; Lecroq et al., 2011). The forambarcoding database is for identification at species level and is based on a partial sequence of six foraminifera-specific hypervariable expansion segments from the 3' end of the SSU (1,000 -1,200 nt), which is used as the “barcode” for foraminifera (Pawlowski and Holzmann, 2014). This database includes only specimens for which both molecular and morphological data are available, although high-resolution SEM images are not always shown. The 37f database is based on a very short fragment (~100 bp), covering the 37f variable region of the SSU. This database allows for taxonomic assignment of environmental DNA sequences amplified via next-generation

sequencing methods. Both databases are curated and although being added to continuously, are still lacking total assemblage coverage and hence require additional data.

The aims of this study were first to gain a more comprehensive understanding of the genetic diversity and biogeography of *Ammonia* within the Northeast Atlantic shelf seas. We sampled living *Ammonia* specimens from 22 locations across the NE Atlantic Ocean margins to establish their biogeographic ranges, to determine their propensity to co-occur and to investigate their potential cryptic nature. All individual specimens were SEM imaged and the range of SSU barcodes determined for each genetic type identified. We subsequently linked these SSU genetic types to the T-type nomenclature already established for *Ammonia*, to avoid multiple and confusing genetic nomenclature. Using an integrated approach, we carried out morphometric analysis on individual, genotyped tests to identify any distinguishing morphological criteria. Where discriminant features were recognised, we described genetic type morphotype profiles and linked them to formally named holotypes. Where morphological features were more gradational between genetic types, the creation of genetic type morphotype profiles were not possible, and we discuss the taxonomic and ecological implications of this.

2. Materials and Methods

2.1 Sampling

Within this project, our sampling strategy was to include the wide range of shelf provinces and biomes found within the middle to high latitude regions of the NE Atlantic. The biogeographic classification of the shelf and upper continental slope is shown in Fig. 1, which follows the most recent biogeographic classification produced for the Oslo and Paris Conventions (OSPAR) Maritime Area (Dinter, 2001). We collected samples from 33 major sampling locations ranging from Svalbard to Portugal. Twenty-two yielded *Ammonia* specimens (Fig. 1; Table 1). Samples containing *Ammonia* were collected from intertidal and subtidal habitats of south Scandinavia, the British Isles and the Dutch, French and Portuguese margins. Intertidal samples were collected by taking a mud scraping from the surface sediment including the flocculent layer and seaweeds were brushed in seawater to detach the foraminiferal tests. For comparisons of the *Ammonia* genetic types and abundances along a transect, equal volumes (38 cm^3) of surface sediment were taken with a cylinder corer, down to 1 cm, at upper-, mid-, and lower-shore sites. Subtidal samples were collected either by SCUBA diving or by deployment of coring devices. All sediments and seaweeds were stored at 4°C prior to processing.

2.2 Identification of live specimens, SEM imaging, and DNA extraction and amplification

Live *Ammonia* specimens were identified and processed through SEM imaging of both umbilical and spiral views, DNA extraction, PCR amplification and cloning as described by Darling et al. (2016). Cloning was performed to ensure accurate designation of genetic types, as intra-individual variation is common within *Ammonia* (Pawlowski, 2000). Individuals were given a unique identification number, which was used at each progressive stage of the SEM image, DNA extraction, amplification and sequencing process.

2.3 Genetic characterisation via sequencing and screening of partial SSU sequences

Sequencing was carried out according to Darling et al. (2016) using a BigDye Terminator v3.1 cycle sequencing kit (Applied Biosystems) and an ABI 3070 DNA sequencer (Applied Biosystems). Once we confirmed genetic type boundaries by DNA cloning and sequencing, we adopted two further approaches to speed up genetic characterisation. The first was to use a short sequence only (the first ~100 bp) which sits within the foraminiferal variable region 37/f (Pawlowski and Lecroq, 2010) providing that it clearly defined the genetic type. The second approach was to use a screening method by designing SSU genetic type (S-type) specific primers to use in conjunction with s14F1 in the secondary PCR using the same PCR conditions (Darling et al., 2016), to give products of different sizes depending on genetic type. We designed primers for the most common S-types in our dataset as follows. S1: 5'-acgcacgatacgcatacacaa -3' (product ~ 530bp). S2: 5'- gacacacgcctgtcgttaaac -3' (product ~280bp). S5a required a mix of three primers to account for the intra-individual variation, S5a-1: 5'-gcccgaaggtgcaacgy-3', S5a-2: 5'-cgtgctcgagagcaacgy-3' and S5a-3: 5'-acctccgaagagagcaacgt-3' (product ~100 bp). S6: 5'-gcgagtaccgaaatacgccg-3' (product ~390 bp). We confirmed that primers were type-specific by performing PCRs with the correct *Ammonia* genetic type, other *Ammonia* genetic types and with other foraminiferal species.

2.4 Amplification and sequencing of the partial LSU sequences

In order to compare our findings with previous studies based on LSU sequences (Hayward et al. 2004; Pawlowski and Holzmann, 2008; Saad and Wade, 2016) we assigned a T-type to our samples. We achieved this by searching GenBank for individuals sequenced for both LSU and SSU genes (e.g., Holzmann et al., unpublished; Schweizer et al., 2011a, 2011b). In addition, we sequenced both the partial SSU and the 5' end partial LSU genes of selected specimens across the range of genetic types collected during this study. Amplifications of the partial LSU sequences were performed with the same PCR conditions as the partial SSU (Darling et al., 2016) and with primers 2TA and LO (Pawlowski, 2000) for the primary PCR followed by 2TAbis (5'-gatacgcgctaaacttaaaca-3') and L10r (5′-aacgatttgcacgtcag-3′) in the

secondary PCR. We aligned partial LSU and SSU sequences from the same individuals in two separate alignments as described in Section 2.5 to link the LSU sequences with SSU sequences and determine the T-types.

2.5 Phylogenetic analyses based on partial SSU gene sequences

The partial SSU sequences from this study were edited in ChromasPro v1.5 (Technelysium Pty Ltd) and aligned manually in BioEdit v7.0.9.0 (Hall, 1999). To obtain a full global picture of *Ammonia* diversity, we also included into the alignment all *Ammonia* partial SSU sequences present in the GenBank database in April 2015 (Supplementary Table S1). From an alignment of 1,143 nt sites, 904 sites could be unambiguously aligned for phylogenetic analysis. Sixteen potential groupings were identified in the alignment and a selection of full-length sequences representative of each group were chosen for analyses (Table 2). No outgroup was used in order to maximize the number of alignable sites available for analyses; phylogenetic trees were therefore unrooted.

Phylogenetic trees were constructed using three different methods. A Bio Neighbor-Joining (BioNJ) tree (Gascuel, 1997) was built using Seaview 4 (Gouy et al., 2010) with 1,000 bootstrap (BS) replicates. Maximum likelihood (ML) analysis was performed with 1,000 BS replicates (Felsenstein, 1985) using PhyML (Guindon and Gascuel, 2003) implemented in Seaview 4. Finally, Bayesian analysis (BA) was built with MrBayes 3.2 (Ronquist et al., 2012). Two independent analyses were done at the same time with four simultaneous chains (one cold and three heated) run for 10,000,000 generations, and sampled every 1,000 generations with 2,500 initial trees discarded as burn-in after convergence was reached. The posterior probabilities (PP), calculated during the BA, estimated the reliability of internal branches. The evolutionary models selected were Kimura 2 parameters or K2P (Kimura, 1980) for BioNJ, Hasegawa, Kishino and Yano or HKY (Hasegawa et al., 1985) and General Time Reversible or GTR (Tavaré, 1986) for ML. A mixed model was used for BA that sampled across the GTR model space (Huelsenbeck et al., 2004). To correct for among-site variations, the alpha parameter of gamma distribution (Γ), with four rate categories, was calculated by Seaview (HKY+Γ, GTR+Γ) and MrBayes.

2.6 Morphometric analysis

2.6.1 Image preparation and measurement of morphological characteristics

To investigate whether the genetic types could be distinguished based upon their morphology alone, a combination of 25 morphological test characteristics were acquired from 316 SEM images of both the umbilical and spiral sides of 158 individual *Ammonia* specimens (Table 3).

The morphological characters measured were primarily derived from Hayward et al. (2004) with some minor modifications and omissions. For example, morphological characteristics such as foraminiferal test area and test roundness measurements were calculated following the methods set out by Roberts et al. (2016). The range of measurements of each morphological test characteristic within each genetic type is documented in Supplementary Table S2. All morphometric measurements for each specimen are available in Supplementary Data 1.

Specimens were excluded if >10% of the test was obscured/damaged or if the specimen had not been imaged from both the umbilical and spiral views. In situations where <10% of the test was obscured/damaged, an infilling procedure was conducted following the methods of Hayward et al. (2004). The morphological data were standardised by ranging the variation between each character from 0 to 1, following the methods of Hayward et al. (2004).

2.6.2 Multivariate data analysis

An unweighted pair-group method using arithmetic averages (UPGMA cluster analysis; dendro UPGMA, Garcia-Vallve et al., 2010) and principal coordinate ordination analysis (PCO; PAST version 2.17, Hammer et al., 2001) were used to assess the utility of the 25 morphological characters in delineating the genetic types within the 158 specimens processed, without *a priori* knowledge of genetic groupings. A discriminant function analysis (DFA) was calculated from the results of the standardised dataset to establish the key diagnostic criteria that can be used to aid classification of specimens into each genetically distinct group. T3V was excluded from the DFA multivariate classification procedure because only two specimens were available for morphological analysis within this genetic subtype. The robustness of the assignment is assessed through a resampling cross-validation procedure in SPSS v.22. The morphological characteristic of presence of dorsal opening, although the main morphological criterion used to distinguish T3 from T15"by eye" (Fig. 2), was excluded from this analysis because it did not exhibit enough variance between the genetic types.

3. Results

3.1 Genetic characterisation based on the SSU and phylogenetic analyses

In total, 378 *Ammonia* individuals were SEM imaged and genetically characterised in this study using the partial SSU, via either cloning and sequencing, or screening methods (Supplementary Table S3). Of these, 233 individuals were sequenced, of which 59 have been cloned (between 2-12 clones each) to determine the number of genetic types and the degree of intra-individual variation. The remaining 145 specimens were fast screened with S-Type-specific primers (Section 2.3). Altogether, 388 new partial SSU sequences were produced and

deposited in the GenBank database (accession numbers: MH124763-MH125150), with supplementary information (e.g., SEM images) deposited in the database "foramBARCODING" (http://forambarcoding.unige.ch). SEM images of representative individuals for each genetic type are shown in Fig. 2.

For phylogenetic reconstruction, the sequences generated in this study were manually aligned together with 87 other *Ammonia* SSU sequences retrieved from GenBank (see methods, Supplementary Table S1). The sequences separate into 16 discrete groups within the alignment, of which six were identified within the NE Atlantic, one of which was further split into two subtypes. The NE Atlantic groups were assigned the S-type identifiers S1, S2, S3, S4, S5a, S5b, and S6. The remaining ten groups occur outside the study area in Japan, Israel, USA, Cuba, Australia, New Zealand and New Caledonia.

A total of 73 partial SSU sequences were used for phylogenetic analyses (46 from GenBank and 27 from this study). All sequences used for phylogenetic analyses are listed in Table 2. The evolutionary relationships among *Ammonia* were inferred using the BioNJ method with the K2P model (Fig. 3). The general topologies retrieved using BioNJ, ML-HKY+Γ, ML-GTR+Γ and BA were slightly different (see Supplementary Figs. S1-S3, respectively). These discrepancies can be explained by the low phylogenetic signal resulting from the relatively limited number of informative sites in the dataset. The statistical support for the BioNJ, ML-HKY+Γ and BA trees is shown at the nodes of the BioNJ tree (Fig. 3).

Sixteen genetic types previously identified in the alignment were also retrieved in the phylogenetic analyses (Figs. 3 and S1-S3). The genetic types represented by more than one sequence formed monophyletic clades with high statistical support (> 85% BS or 0.85 PP), except for S2, which exhibited either low support (BioNJ: 66%, ML-HKY+Γ: 44%) or was paraphyletic with S3 (ML-GTR+Γ, BA). Within the alignment, S5 can be divided into the two subtypes, S5a and S5b. They were given subtype ranks since their sequence differences are significant but small. Further sampling would improve their characterisation, but there is currently not enough phylogenetic signal in the 1,143 nt site alignment used in this study to fully separate them into two discrete phylogenetic clades (Figs. 3 and S1-S3).

The relationships between the genetic types are more difficult to assess, as the deeper nodes have low support and the branching patterns sometimes vary between analyses (Figs. 3 and S1-S3). Nevertheless, some groupings are more stable than others. S5a and S5b are closely related subtypes and group together (98/42/0.87). They also form a highly supported group (99/85/82/0.88) with S6 in all analyses. The genetic types S2 and S3 are also closely related

with high statistical support (100/96/98/1.00). The two clades (S5-S6 and S2-S3) fall on a common but unsupported branch, but cluster closer to each other than to either S1 or S4 in the phylogeny. Genetic types S1 (100/100/1.00) and S4 (100/90/0.99) are both well supported clades in the unrooted tree.

3.2 Linking SSU to LSU sequences and the T-type nomenclature used in the genetic characterisation of Ammonia

Genetic characterisation of *Ammonia* utilising the LSU has yielded 13 genetic types, designated T1-T13 (Hayward et al., 2004). In order to avoid confusion, since the LSU T-type nomenclature is already established, we have linked our S-types S1-S6 directly to the LSU nomenclature. A GenBank search revealed that 37 individual specimens had previously been characterised for both their LSU and SSU genes (Hayward et al., 2004; Schweizer et al., 2011a, 2011b). Among them, 19 represent the S-types S1, S2, S4, S5a and S6 identified in this study. In addition, we sequenced individual specimens of S-types S2, S3, S4, S5a and S5b for both genes, (LSU accession numbers: MH136606-MH136620) to obtain their equivalent T-type and also to supplement the available GenBank data (Supplementary Table S4).

Separate alignments of all the SSU and LSU sequences from the same individuals revealed that the same six clades of *Ammonia* can be recognized in both genes. Two SSU genetic types and two subtypes from this study can be directly assigned to a previously defined T-type (Hayward et al., 2004). These convert to S1=T6, S4=T1, and the two subtypes S5a=T3S and S5b=T3V (Table 4). Allocation of a T-type to S2 and S3 is more complex because specimens containing S2 and S3 SSU sequences have both been previously allocated T2 (Table S1). However, the S2 specimens incorporate the T2 LSU sequences, whilst on close inspection, those of S3 differ (Supplementary Data 2). Despite being very closely related, the variable units in our S2 specimens were not found in the S3 specimens and vice versa indicating genetic distinction. However, S2 and S3 cannot always be separated in phylogenetic analysis (Figs. 3 and S1-S3), since we use a conservative alignment which does not include the variable units which characterise them (Section 2.5). A more comprehensive sample survey with extensive cloning is required to fully understand the relationship between S2 and S3. We have therefore assigned them to subtypes T2A (S2) and T2B (S3) until their relationship can be fully resolved. In addition, we have allocated T14 to a previously undesignated Australian genetic type (Fig. 3; Schweizer at al. 2011a), and finally T15 is allocated to S6. The established T-type nomenclature (Table 4) will be used for all further results and discussion.

subtypesubtype*3.3 Morphological analysis of the* Ammonia *genetic types*

A combination of 25 morphological test characteristics (Table 3) were determined from the SEM images of both the umbilical and spiral sides of 158 individual *Ammonia* specimens for multivariate data analysis. The range of measurements of each morphological test characteristic within each genetic type is documented in Supplementary Table S2. UPGMA cluster analysis and PCO analysis were employed to assess the utility of morphology as a tool for *Ammonia* classification without *a priori* knowledge of genetic groupings. A DFA was then performed on the dataset utilising our knowledge of the genetic types, to assess the effectiveness of morphological traits in predicting genetic type membership and to identify the diagnostic value of the morphological features analysed.

3.3.1 UPMGA analysis

The UPGMA cluster analysis demonstrates that genetic types T3S, T3V, and T15 are morphologically distinct from genetic types T1, T2A, T2B, and T6, as they form discrete clusters within the morphology dendrogram (Fig. 4). In comparison, no clear clustering patterns were identified between the less ornate genetic types T1, T2A, T2B and T6, as they exhibited extensive morphological overlap between the individual specimens (Fig. 4).

3.3.2 PCO analysis

The primary PCO analysis demonstrates similar results to the UPGMA cluster analysis. Genetic types T3S and T3V can clearly be distinguished from genetic types T1, T2A, T2B, T6 and T15 in the PCO morphospace (Fig. 5). In addition, despite low numbers of T3V specimens, T3S and T3V can also be separated from each other. However, unlike the UPGMA cluster analysis (Fig. 4), T15 is not separated from the less ornate genetic types within the PCO morphospace (Fig.5).

In order to clarify the validity of the morphological separation of genetic type T15 within the UPGMA analysis (Fig. 4), a refined PCO analysis was performed. This analysis omitted the specimens from genetic types T3S and T3V because they were clearly separated by the primary PCO analysis and the UPGMA dendrogram (Figs. 4 and 5). The refined PCO analysis illustrates that genetic type T15 specimens form a discrete non-overlapping cluster, clearly distinct from the PCO morphospace occupied by genetic types T1, T2A, T2B and T6 (Fig. 6), in agreement with the UPGMA analysis. This extended multivariate morphological analysis also reveals that no other genetic type can be clearly delineated, as substantial morphological overlap is observed between genetic types T1, T2A, T2B and T6 within the PCO morphospace (Fig. 6). Although it should be noted that whilst specimens of genetic types T1 and T2B are completely encompassed within the morphospace of genetic types T2A and T6, they do not exhibit any overlap with each other (Fig. 6).

3.3.3 Discriminant function analysis (DFA)

Genetic type T3V was excluded from the DFA multivariate classification procedure, again (see 2.6.2) because only two specimens were available for morphological analysis within this genetic type. The DFA reveals that in total 98.1% of *Ammonia* specimens were correctly classified into their genetic type, based upon their morphological test characteristics and that 90.4% were correctly assigned after the cross-validation procedure (Wilks: -0.001, significance p: <0.001). From a total of 156 specimens, three *Ammonia* specimens were misclassified in the DFA, and 15 specimens were misclassified in the cross-validation analysis (Table 5).

Genetic type T3S exhibits the highest assignment success based upon morphology, as all specimens were correctly classified in both the DFA and cross validation procedures. In addition, no other genetic types were misclassified into this genetic type (Table 5). Specimens of genetic type T15 also exhibit perfect discrimination in the DFA based upon their test morphology. However, the cross-validation procedure illustrates that four specimens of genetic type T15 were incorrectly classified into other genetic types. This misclassification could be explained by the omission of a key discriminatory variable (presence of secondary dorsal openings) from the DFA, because it did not exhibit variance between the groups. This suggests that even with the exclusion of a key morphological trait, this genetic type can be successfully discriminated from other *Ammonia* genetic types based on its other characteristics of test morphology.

In contrast, the results of the DFA and cross validation procedure indicate that morphological separation between the less ornate genetic types T1, T2A, T2B and T6 is more challenging. Whilst genetic type T2A exhibited perfect discrimination in the DFA and cross-validation procedure, two specimens of T6 and four specimens of T2B were misclassified into this genetic type. Although the DFA illustrates that 87.5-100% of specimens of genetic types T1, T2B and T6 can be correctly classified, only 25-92% of specimens were classified into their correct groups in the cross-validation procedure. In addition, the misclassification of specimens is evenly distributed between the three genetic types (Table 5). This indicates that the interspecific morphological boundaries determined in this study between genetic types are not discrete and are gradational in nature. However, no morphological overlap was observed between genetic types T1 and T2B, suggesting that it may be possible to separate these genetic types from one another based on morphology. The key diagnostic morphological variables identified by the DFA include a combination of ornamentation and structural features. These are development of thickened calcite on the spiral side (24), development of beads and grooves along the edge of the suture (10, 11), porosity features including pore

density and pore diameter (5, 20, 21), degree of thickened calcite on folia (8), the development of radial sutural furrows (23), proloculus diameter (22), and test roundness (17). The morphological traits in brackets correspond to the characters described in Table 3.

3.4 Biogeography, depth and habitat preferences of Ammonia *genetic types in the NE Atlantic*

The biogeographical distribution of each genetic type identified in this study is described in Table 6 and accompanied by individual distribution maps (Figs. 7 and 8). Depth and habitat preferences for each of the genetic types are described in Tables 1 and 6. At Dartmouth (location 18), three different *Ammonia* genetic types (T1, T2A, and T3S) were found in a single sediment sample taken from the lower-shore sampling site (Table 1). To determine whether this was consistent across the whole of the intertidal zone or whether different genetic types dominated different areas of the shore, we collected three sediment samples of equal volume (38cm^3) along a transect from the upper-, mid- and lower-shore, to genetically characterize the living *Ammonia* profiles. The results show increasing numbers of individuals and genetic types from the upper- to the lower-shore (Table 1; Fig. 9). On the upper shore, T2A comprised 100% of the *Ammonia* assemblage, but only six *Ammonia* specimens were found in total. On the mid-shore, of 15 specimens, T2A made up 80%, whilst T3S contributed 7% of the assemblage and T1 accounted for 13%. On the lower shore, T2A again dominated the assemblage comprising 75% of the 65 *Ammonia* specimens, whilst T3S and T1 made up 22% and 3%, respectively (Fig. 9).4. Discussion

The taxonomy of *Ammonia* is still in confusion, although the seminal study by Hayward et al. (2004) has brought some taxonomic order to this globally distributed genus. Nevertheless, the identification of *Ammonia* specimens remains hugely challenging, due to the cryptic or pseudo-cryptic nature of some genetic types and the perceived wide morphological variation in others. We now present a clear overview of the seven genetic types and subtypes of *Ammonia* identified along the NE Atlantic Ocean margins. For each genetic type and subtype we have provided SSU barcodes (Genbank) linked to SEM images (forambarcoding database) enabling us to deliver the first morphometric analysis on a dataset of fully barcoded specimens.

In agreement with Hayward et al. (2004) and Schweizer et al. (2011a), we demonstrate that genetic subtype T3S and genetic type T15 can be morphologically distinguished. In addition, genetic subtype T3V can also be distinguished by morphometric analysis. However, a larger sample set and further genetic profiling is required to establish this subtype as distinct from T3S. We also provide evidence that the remaining four genetic types/subtypes cannot be robustly delineated 100% of the time with the morphometric analyses performed in this study and, at present, should be considered as cryptic species. However, a semi-automated method

to measure the porosity of *Ammonia* tests presented in other studies (Petersen et al., 2016; Richirt et al. in press) may prove an additional and useful tool for their discrimination.

Following the strict integrated approach proposed by Roberts et al. (2016), it is not possible to assign taxonomic names without adding further potential confusion to the literature. However, the taxonomic allocations made by Hayward et al. (2004) for these genetic types are discussed below. We provide biogeographical distributions of each genetic type within the NE Atlantic margins and ecological information including co-occurrence profiles, which, combined with morphological information, will be helpful in identifying genetic types in the field.

Whilst the sampling regime employed in this study provides a broad overview of the regional distributional patterns of *Ammonia* in the NE Atlantic, it is important to recognise that it is not exhaustive. For example, some of the biogeographic provinces identified in Dinter (2001) have not been sampled, such as the Warm Lusitanean subprovince and the White Sea. Additionally, the Cool Lusitanean and West Norwegian subprovinces have only been marginally sampled (Fig. 1). Nevertheless, the northern limit of *Ammonia* is known (around 60°N), and the bias concerns mainly the southern region. There is also a sampling bias towards intertidal areas. Consequently, the complete genetic and morphological diversity of *Ammonia* species may not have been fully captured in the subtidal areas of focus in this study. In addition to data from the NE Atlantic margins, we report a small dataset from subtidal sampling undertaken in the western Mediterranean Sea, to supplement a large body of intertidal sampling that has been documented in the region (e.g. references in Supplementary Tables S1 and S5). Despite these limitations, the sampling employed in this study presents the most extensive genetic and taxonomic evaluation of *Ammonia* diversity conducted to date within this region.

4.1 Genetic characterisation and molecular phylogeny

As discussed, the T-type nomenclature for the genetic types of *Ammonia* is now well established, despite being based on genetic differences in the LSU rather than the SSU, which is the common practise for the other foraminiferal groups (Pawlowski and Holzmann, 2014). Therefore, to avoid multiple and confusing nomenclature, a primary aim of this study was to bring the T-type nomenclature in line with the molecular characterisation of other foraminiferal groups and to generate SSU barcodes for database submission.

4.1.1 **Ammonia** *rRNA gene arrays*

Ammonia genetic types were initially characterised by direct comparison of SSU sequences within a 1143 nucleotide site alignment, of which only 904 bp could be unambiguously

aligned for use in phylogenetic analysis. Examination of the unalignable variable regions of the SSU 3' fragments (e.g., Schweizer et al., 2008; Pawlowski and Lecroq, 2010; Weber and Pawlowski 2014), showed that five out of the six SSU genetic types identified in the study area contained several different gene copies. However, the variable units observed within and between individuals were unique to each genetic type, including between the closely related subtypes T2A and T2B. In contrast, T3S and T3V have one shared variable unit. The presence of multiple gene copies within the SSU gene variable regions in *Ammonia* is consistent with our data on elphidiid genetic types (Darling et al., 2016), and with work done specifically on a Patagonian *Elphidium* species (Pillet et al., 2012), together with other foraminiferal species belonging to the rotaliids, textulariids and allogromiids (Weber and Pawlowski, 2014). Multiple gene copies were also observed previously in the LSU of *Ammonia* (Holzmann et al., 1996), confirming that this is a common phenomenon in the rRNA gene arrays of the benthic foraminifera. We used a representative set of SSU gene copies to define each genetic type, with the exception of genetic type T1, for which only one gene copy was found within the eight specimens collected in our study area. However, T1 has a cosmopolitan distribution (Hayward et al., 2004) with a wide range of variable units within its SSU sequences (Fig.3; Table S1), and the New Zealand T1 sequence (HE598562) has identical units to those of our T1 sequences, confirming its identity.

4.1.2 Phylogenetic analyses based on SSU sequences

The *Ammonia* genetic types T1, T2, T3S, T3V, and T6 identified within our study area, were first recognised by Holzmann and Pawlowski (2000). However, we further divided T2 into two subtypes in this study (T2A and T2B), as there was some degree of support for their separation in the SSU NJ phylogeny. The clade T2B is always well supported (BioNJ: 99%, ML-HK: 94%, ML-GTR: 96%, BA: 1.00), whereas the clade T2A has either a low support (BioNJ: 66%, ML-HKY: 44%; Fig. 3; Fig. S1), or does not exist (ML-GTR, BA; Fig. S2-S3). The possibility of two potential subtypes of *Ammonia* T2 was mentioned in Holzmann and Pawlowski (2000) and later Weber and Pawlowski (2014) also suspected the presence of an additional genetic type within the T2 clade. The designation T15 was also allocated to the SSU genetic type S6, which was identified within our study area. This genetic type had previously been morphologically identified as the species *A. falsobeccarii* (Rouvillois, 1974; Schweizer et al., 2011a). Six of the *Ammonia* SSU genetic types (T1, T2A, T2B, T3, T6, and T15) were well supported in the NJ phylogeny (Fig. 3). However, the very closely related genetic subtypes T3S and T3V were not well supported, as the SSU phylogenies produced from our conservative alignment do not fully resolve them (Supplementary Data 3). Nevertheless, they show sufficient difference in their variable regions to be considered subtypes, and these sister genetic types were already split and allocated to T3S and T3V by

Hayward et al. (2004) based on their LSU sequences (See Supplementary Data 2 for LSU alignment of T3S and T3V). Investigation of the hypervariate rRNA internal transcribed spacer (ITS) region of these two genetic types, in combination with additional T3V specimens sampled and cloned from other locations, may shed more light on their phylogenetic relatedness.

One divergent clade within the phylogenetic tree (Fig. 3) includes two sequences from Lizard Island on the East coast of Australia (Schweizer et al., 2011b). We have designated this genetic type T14, since it has not previously been assigned. Interestingly, it has not yet been identified across the Coral Sea in New Caledonia where T1, T12 and T13 were all found. However, Hayward et al. (2004) reported six distinctive *Ammonia* morphotypes within the sediments there, suggesting that there are three types still to be sequenced. Whilst it is important to note that some of these morphotypes might be present as a result of post-mortem transport, it is also plausible that T14 is one of these New Caledonia morphotypes that are yet to be sequenced.

4.2 Morphological discrimination of **Ammonia** *genetic types and cryptic diversity*

This study is the first morphometric analysis performed on a dataset of fully genotyped specimens including the complete range of *Ammonia* genetic types identified along the NE Atlantic margins. These are T1, T2A, T3S, T3V and T6, which were also analysed by Hayward et al. (2004), plus T2B and T15, which were not analysed in the 2004 study. In total, 316 SEM images from 158 specimens were used in morphometric analyses. Using a range of statistical analyses, we have directly compared the interspecific taxonomic boundaries identified by quantitative morphological analysis, against the seven distinct genetic types and subtypes from the NE Atlantic.

4.2.1 Morphologically resolved genetic types

Genetic subtypes T3S and T3V can be robustly distinguished from genetic types T1, T2A, T2B and T6, using a combination of structural and ornamental test characteristics (Table 3; Supplementary Table S2). Interestingly, although only limited genetic divergence has been identified between T3S and T3V (Fig. 3; Supplementary Data 2 and 3), they exhibit clearly distinctive morphologies (Figs. 2, 4 and 5), providing substantial support for their potential genetic distinction. T3S can be distinguished based on a combination of morphological characters, including the development of thickened calcite over the spiral central area (Fig. 2). This species also typically exhibits a more pronounced development of the radial sutural furrows than specimens from genetic subtype T3V (Supplementary Table S2). In addition, T3S commonly possesses a number of umbilical bosses (0-3). In contrast, T3V lacks a

distinctive umbilical boss. Instead, T3V seems to be distinguishable from T3S by its stronger development of beads and grooved notches on the umbilical side, which sometimes extend all the way to the periphery of the test (as depicted in Fig. 2; Supplementary Table S2). T15 can be discriminated by a single discrete morphological test trait that is the presence of secondary dorsal openings (Fig. 2; Schweizer et al., 2011a), illustrating the effectiveness of morphology as a tool for species delineation in these genetic types.

4.2.2 Morphologically cryptic genetic types

The remaining four *Ammonia* genetic types (T1, T2A, T2B and T6) have significantly fewer discriminating characteristics. They overlap in the PCO morphospace, in the UPGMA cluster analysis tree, and even though T2A was correctly assigned to its genetic type 100% of the time in the DFA cross validation procedure (Figs. 4, 5 and 6; Table 5), other genetic types (T6 and T2B) were misclassified as T2A. These genetic types exhibit gradational test characteristics, i.e., the morphological boundaries between them are not discrete (Supplementary Table S2). They exhibit the least test ornamentation, possess a broadly rounded periphery and have a similar number of visible test chambers per whorl (Supplementary Table S2).

Genetic type T6 has the largest average pore diameter (mean diameter 1.0-4.23 μm on the spiral side and 1.39-8.64 μm on the umbilical side, (Supplementary Table S2). However, the average pore sizes of end members of T1, T2A and T2B all overlap with T6, with the exception of T2B on the umbilical side, where average pore size is smaller (there is overlap on the spiral side). In contrast to T6, genetic type T2A commonly has smaller pores (mean diameter 0.51-1.26 μm on the spiral side and 0.33-2.02 μm on the umbilical side), but higher pore density (4-28 pores per 100 sq. μm). Hayward et al. (2004) suggested that T2 can be distinguished from T1 and T6 by its small pores. However, our analysis shows significant overlap with other genetic types in the PCO morphospace (Fig. 6), and misclassifies T6 as T2A in the cross-validation procedure (Table 5). In addition, we have split T2 into T2A and T2B in this study, and T2B commonly has the smallest pore diameters (e.g., mean pore diameter 0.39-0.87 μm on the umbilical side). Both genetic types T6 and T2A also sometimes display the development of small pustules along the edges of umbilical sutures (often extending to the periphery) and ornamentation on the folia, which can help to distinguish them from genetic types T1 and T2B, which rarely exhibit these characters. Genetic type T1 typically exhibits slightly lower pore density in contrast to the other three *Ammonia* genetic types (T1: 6-8 pores per 100 sq. μm; T2A: 4.76-29.40 pores per 100 sq. μm; T2B: 6.06-17.35 pores per 100 sq μm; T6: 0.56-11.35 pores per 100 sq. μm; Supplementary Table S2), together with a fissure on the spiral side (Fig. 2), although this feature is not always strongly

developed. T1 also rarely possesses a small umbilical boss, being often depressed in the umbilical region and exhibiting very weak to weak secondary calcite on the spiral area (Supplementary Table S2). Interestingly, in the Lagoon of Venice, where both T1 and T2B have been observed, Holzmann and Pawlowski (1997) reported being able to distinguish "with difficulty" the two distinct genetic types, based on pore parameters and test size. Our morphometric analysis supports this, as T1 and T2B do not overlap in the PCO morphospace (Fig. 6). Pore parameters are one of the key diagnostics in morphometric analyses of the less ornate *Ammonia* genetic types (Hayward et al., 2004; this study). Studies using the semi-automated method to measure the porosity (percentage of surface in the measurement frame covered by pores) of *Ammonia* tests (Petersen et al., 2016; Richirt et al., in press) have discriminated T1 and T6 from T2A/B but T2A and T2B remain morphologically indistinguishable. In the literature, porosity is currently explained either by genetic differences (e.g., Morard et al., 2009; Schweizer et al., 2009; Petersen et al., 2016) or ecophenotypic variations (e.g., Glock et al., 2011; Kuhnt et al., 2014; Petersen et al., 2016; Roberts, 2016). However, with the exception of Roberts (2016), those studies promoting ecophenotypic variations to explain porosity differences, used non-genotyped individuals. Hence, in these studies a genetic basis for changes in porosity cannot be ruled out. The work by Roberts (2016) however, does provide some evidence for ecophenotypic variation of pore size. *Ammonia* T6 specimens from Hanö Bay (location 7) had significantly larger pore size than T6 specimens from Norfolk (location 13), Laugharne Castle (location 14) and Cardiff (location 17). The major difference between these four sites is that the *Ammonia* T6 specimens were sampled from low salinity (7-13) subtidal waters at Hanö Bay as opposed to intertidal mudflats at all other locations. In addition, the Hanö Bay specimens demonstrated significant signs of etching, which may have contributed to the larger pore sizes, and more studies are required therefore, to determine habitat influence on pore size.

This study shows that genetic types T1, T2A, T2B and T6 are partially cryptic due to overlap of endmembers. Whilst some key diagnostic morphological variables were identified (Section 3.3.3), no diagnostic features were found in this study to consistently delineate between these genetic types. This indicates that the less ornate genetic types are practically cryptic in an applied taxonomic situation. These results underscore the necessity for employing multiple lines of evidence (such as DNA, ecology, morphology, and biogeography) for re-evaluating taxonomic boundaries within this genus, because at present, morphology alone is insufficient for elucidating diversity. This is illustrated by a recent morphometric study focusing on the morphology of sequenced genetic types T1, T2A/T2B together and T6, which has successfully discriminated these three groups on the basis of morphological criteria observable with a stereomicroscope (Richirt et al., in press).

4.2.3 Comparative morphometric studies in **Ammonia**

Hayward et al. (2004) found that all molecular types could be discriminated based on their morphology, although end members were hard to distinguish from each other. Superficially, this appears counter to our findings, as our study suggests that there is morphological overlap between end members that make some genetic types partially cryptic. However, previously unrecognised genetic diversity could account for some of the differences in the morphological boundaries observed between our study and those of Hayward et al. (2004). In particular, the splitting of T2 into T2A and T2B, has increased the difficulty in delineating these small less ornate genetic types. T2B is entirely enclosed within the morphospace of T2A and overlaps with T6 (Fig. 5), and 25% of T2B specimens are misclassified as T2A in the DFA cross validation procedure (Table 5). The interspecific morphological boundaries identified for T2 by Hayward et al. (2004) will therefore encompass the morphological characters of T2B.The differences in the morphological boundaries identified between this study and those of Hayward et al. (2004) may also be the product of the different morphological characteristics analysed. For example, this study measured 23 out of the 37 morphological characters originally assessed by Hayward et al. (2004), and a number of these variables were slightly modified. We also utilised computer-aided techniques to standardise the measurements of several morphological characteristics, thereby reducing human subjectivity. One of the morphological characteristics not measured in this study, but measured by Hayward et al. (2004) is the development of the protoforamen. Hayward et al (2004) determined that T1 always possesses a protoforamen that is often strongly developed. Measuring this characteristic might help in discrimination of T1. Nine of the morphological features used by Hayward et al. (2004) that were omitted in this study were due to the unavailability of SEM images taken from the profile aspect of the foraminifera. Therefore, the taxonomic re-evaluation of the morphological boundaries of *Ammonia* presented in our study might not have captured all the key diagnostic traits. For example, Hayward et al. (2004) identified that the profile diameter is a strong diagnostic character, thus the inclusion of this feature in future investigations may help to discriminate between cryptic specimens.

4.3 Nomenclature and taxonomy

The genetic types defined for *Ammonia* (T1-T15) are thought different enough to be considered as separate species (Holzmann, 2000; Hayward et al., 2004; this study), yet distinct genetic types are not always morphologically discrete (Pawlowski et al., 1995; Holzmann and Pawlowski, 1997; Holzmann, 2000; Hayward et al., 2004; this study). Where morphological variation is observed, the traditional view would have been that they represent ecophenotypic variants of *Ammonia* (e.g., Schnitker, 1974 Jorissen, 1988; Holzmann, 2000

and references therein). However, in agreement with Hayward et al. (2004), the high number of individual specimens genotyped in this study confirms that the morphological differences observed in morphometric analyses are due to genetic distinction and are not a result of environmentally controlled morphological variations. Species names can therefore be confidently allocated to those genetic types that can be morphologically discriminated and match a strict type description. However, several of the genetic types are partially cryptic or pseudo-cryptic (T1, T2A, T2B and T6) and only genetic types T3S, T3V and T15 can be robustly distinguished.

4.3.1 Allocation of species names

Morphospecies names cannot be confidently allocated to genetic types unless both the morphology and genetic type have been linked to a formally named holotype (Roberts et al., 2016). Ideally live topotypes should also be sampled to complete the picture, but this is not always possible. To overcome this issue, a three-stage approach has been proposed to make the genetic/taxonomic link (Darling et al., 2016; Roberts et al., 2016), which incorporates the following steps. (i) Genetic characterisation with high-resolution imaging of the test, (ii) genetic type delineation by generating a morphotype description produced only from the range of test morphologies associated with the genetic type and (iii) allocation of the most appropriate taxonomic name by linking the genetic type morphotype description to a taxonomic morphospecies description, using only strict morphological criteria. Of those species that can be robustly delineated via morphometric analysis, T3S and T15 can be confidently allocated morphospecies taxonomic names using this three-step method. The allocation of T3V as a distinct subtype or species, and hence the allocation of a species name, requires further analysis of additional specimens to confirm the morphological delineation observed here and to determine the uniqueness of the units of intra-individual variation in the rRNA gene arrays.

Genetic subtype T3S description. – Test relatively large, trochospiral, inflated and usually with lobulate periphery, at least in the last part of the final whorl. Between 8 and 12 chambers in the final whorl. On the spiral side, it typically has pronounced development of sutural furrows along both the radial chamber sutures and the spiral suture. These are usually restricted to the later part of the last whorl, but they are sometimes found almost throughout the last whorl. It has often developed thickened calcite over the spiral central area. Relatively strong development of beads and grooved notches are seen on the umbilical side, sometimes extending to the periphery. Usually it has one large umbilical boss, sometimes up to three, but sometimes lacking.

In agreement with Hayward et al. (2004) we link genetic type T3S to the morphospecies *Ammonia batava* (Hofker, 1951). Hofker (1951) described this new species (as *Streblus batavus*) with the North Sea as type locality (Voorne Island, The Netherlands). Hofker (1951) separated *Streblus batavus* from *Ammonia beccarii* (Linné, 1758), i.e., as a smaller and less depressed form, and he discussed in detail the differences between *Streblus batavus* and the type material of *Ammonia beccarii* (Linné, 1758) from Rimini in the Adriatic, including differences in apertural and internal structures.

Genetic type T15 description. – Test relatively large, trochospiral, inflated and typically with lobulate periphery, at least in the last part of the final whorl. Between 7 and 9 chambers in the final whorl. A typical morphological test trait for this genetic type is the development of secondary dorsal openings where the spiral suture meets the radial chamber sutures. In most specimens these openings are only developed along part of the last whorl, but they are often seen throughout the last whorl and sometimes even along part of the second-last whorl. Relatively strong development of beads and grooved notches are seen on the umbilical side, but these are usually restricted to the central area and not extending to the periphery. There is no distinct umbilical boss, but sometimes several minor less well-defined bosses are seen in the central area. This genetic type (T15) can be linked to the morphospecies *Ammonia falsobeccarii* (Rouvillois, 1974; see Schweizer et al., 2011a).

4.3.2 Naming cryptic types of Ammonia

Until the partially cryptic genetic types can be conclusively linked to the morphology of type specimens and allocated taxonomic names, they should be named following the system of Hayward et al. (2004) as *Ammonia* sp. T1, *Ammonia* sp. T2A, *Ammonia* sp. T2B, and *Ammonia* sp. T6, to avoid the taxonomic confusion that is prevalent in the literature. This is of course only possible, if genotyping has been carried out. The allocation of either a T-Type or a species name to any cryptic specimens, without the aid of genotyping is not recommended, but if carried out, must be done with care, and any supporting biogeographic and ecological information should be provided.

Hayward et al. (2004) did apply taxonomic names to a number of the genetic types identified. *Ammonia* sp. T2 has been linked to the taxonomic name *A. aberdoveyensis* Haynes, 1973 (cf. pl. 38, no. 1-2; Holzmann and Pawlowski, 2000; Hayward et al., 2004). Although both T1 and T2 were found at the type locality, T2 was assigned to *A. aberdoveyensis* due to its smaller proloculus in line with the holotype. In this study, we have split T2 into the cryptic types T2A and T2B. Nevertheless, it is T2A that is found at the type locality in the Boreal province, Wales, UK. Although T2B is also found in Wales, it is only found in the Boreal-Lusitanean

province further south and appears to be a warmer water species than T2A. It is therefore possible to retain the name *A. aberdoveyensis* for T2A, with the caveat that T2A and T2B cannot be morphologically delineated with confidence. Biogeographical data can be used to assist identification, as it is unlikely that T2B will be found in the North Sea boreal province, whereas T2A has been identified there. However, in warmer waters they can co-occur (Fig. 7; Section 4.5.2) and hence care must be taken in taxonomic assignment of specimens in warmer provinces.

Hayward et al. (2004) also allocated *Ammonia* sp. T6 the taxonomic name *A. aomoriensis*. Hayward's allocation has led to a number of studies using either genotyping (Schweizer et al., 2011b; Lei et al., 2016) or the taxonomic description (Haynert et al., 2012; Nehrke et al., 2013; Langer et al., 2016) for the allocation of their study specimens to the taxon *A. aomoriensis*. We strongly recommend caution in utilising this taxonomic name. The holotype of *Rotalia beccarii* var. *aomoriensis* is from the Pliocene Hamada Formation (Shimokita Peninsula, Aomori Prefecture, Japan), but the taxon is mentioned by Asano (1951) as also occurring in recent material in northern Japan. It is not possible to sequence Pliocene topotype material. Toyofuko et al. (2004) sequenced T6 from modern assemblages of six localities in the nearby area. However, since the oceanographic conditions would have changed markedly since the Pliocene, it is not valid to allocate *A. aomoriensis* to the genetic type T6, despite T6 being found abundantly in the wider region (Lei et al 2016; Supplementary Tables S1 and S5). In addition, we find a number of discrepancies in the taxonomic description of *A. aomoriensis* (Asano, 1951) and the morphology of the 50 T6 specimens we have imaged by SEM in our morphometric dataset. The original description states that there are 6-7 chambers in the last whorl whereas T6 has 6-11. It states that the wall is "finely perforate" (a rather broad description that can be assigned to almost any type) and "sutures not limbate". However, several of our T6 images show thickened sutures on the spiral/dorsal side. It should be mentioned, however, that the description of *A. aomoriensis* (Asano, 1951) was based on light microscope examination, which may be difficult to compare with SEM observations. We conclude that T6 should not currently be allocated to the taxon *A. aomoriensis* due to morphological discrepancies and a lack of genetic information.

The taxonomic name *Ammonia tepida* (Cushman, 1926) has been widely used in many studies in the NE Atlantic margins and the Mediterranean Sea, as well as globally. The holotype *Ammonia tepida* from the San Juan Harbour (Puerto Rico), which is recorded in the Cushman Catalogue of 1929, has been re-described by Hayward et al. (2003) and designated as a lectotype. Hayward et al. (2003) concluded (using both morphological observations and DNA sequencing) that the *Ammonia tepida* morphotype has a tropical, equatorial distribution,

and that more temperate specimens are of other molecular types and differ in their morphology. We suggest therefore that the taxonomic name *Ammonia tepida* should not be applied to any of the small less-ornate specimens found in in the temperate waters of the NE Atlantic margins.

4.4 The distribution of **Ammonia** *in the NE Atlantic*

4.4.1 Northern boundary of **Ammonia** *morphospecies*

In our study, sampling carried out at the northerly sampling sites at Svalbard and Iceland yielded no *Ammonia* specimens. This is in agreement with previous studies which have no recorded observations of *Ammonia* off Iceland (e.g., Nørvang, 1945; Jennings et al., 2004), in the White Sea (Korsun et al., 2014), off the north coast of Norway, in the Tanafjord (70°N; Corner et al., 1996) or slightly further south at Malangenfjord (69°N; Husum and Hald, 2004). The most northerly occurrences of *Ammonia* recorded in the literature were identified in the shallow subtidal areas of the Bergen fjords (Austin and Serjup, 1994; Murray and Alve, 2016). In this study, we also sampled off Bergen, (60°N), but found no *Ammonia* specimens amongst the 271 foraminifera collected there. The most northerly *Ammonia* specimens found in our study were in subtidal samples from the Shetland Islands. No specimens were found here in the intertidal sediments examined, either alive or dead. It is most likely that the near-shore populations of *Ammonia* decline to zero between Bergen (60°N) and Malangenfjord (69°N), and therefore the northern limit of *Ammonia* lies within this region in the present day. Additional sampling in the region would confirm its more exact location. Poole and Vorren (1993) did find *Ammonia* specimens in sediments from the mid-Norwegian shelf (65°- 66°N), but these were fossil foraminifera dating from the Pliocene, a period which was warmer than today (Zachos et al., 2001). We therefore conclude that the most northerly *Ammonia* populations, are currently found at the northern boundary of the Boreal province and in the southern part of the West Norwegian subprovince (Fig. 1).

4.4.2 Regional distribution of **Ammonia** *morphospecies*

The distribution of *Ammonia* in the NE Atlantic has been summarised as present from southern Norway to Portugal (Murray, 2006). *Ammonia* has been shown to be prevalent in both the Skagerrak and Kattegat margins (Alve and Murray, 1999; Holzmann and Pawlowski, 2000), down to depths of 70 m (Conradsen, 1993; Conradsen et al., 1994; Bergsten et al., 1996). It has also been observed down to depths of 120 m in the Oslofjord (Risdal, 1964; Alve and Nagy, 1990; Alve and Goldstein, 2003). It is perhaps surprising then, that we did not find any subtidal *Ammonia* genotypes in the Skagerrak subprovince, where we collected large numbers of foraminifera (299 specimens adjacent to the Gullmar Fjord (119m); 859 specimens from Oslofjord (22-202 m)). In this study, the first regional sediment samples

containing *Ammonia* specimens were collected further south in the Kattegat at Anholt (location 6) in the Boreal province and perhaps unexpectedly in the southern Baltic at Hanö Bay (location 7), where *Ammonia* was thought to be absent (Hermelin, 1987; Murray, 2006: p. 66). However, in 1965 Lutze reported its presence in the eastern boundary of the Arkona Basin adjacent to Hanö Bay (location 7) at salinities of 15. In this study, we have found *Ammonia* to be present along the length of the Atlantic European continental margin and into the Mediterranean (Figs. 1, 7 and 8), consistent with the literature (e.g., Pawlowski et al., 1995; Holzmann and Pawlowski, 2000; Hayward et al., 2004; de Nooijer et al., 2009; Dissard et al., 2010; Foster et al., 2012; Frontalini et al., 2015; Saad and Wade 2016; LeKieffre et al., 2017; Koho et al., 2018; Tables S1 and S5 and references therein). We therefore consider the genus to be ubiquitous in Europe south of 60°N.

There are differences in the abundance and distribution of *Ammonia* between the biogeographical provinces. For example, the continental margins of the North Sea, including the east coast of Scotland, are within the Boreal province, a slightly cooler biome than found on the west coast of Scotland, which is bound by the Boreal-Lusitanean province. This west coast province is characterised by warm waters deriving from the North Atlantic Drift, and is a province of enhanced marine biodiversity, where warm water species appear at comparably high latitudes than in the east (Mitchell et al., 1983; Dinter, 2001; Hiscock and Breckels 2007). This is also observed in our sample set. *Ammonia* was found abundant at latitudes of around 56°N at Torry Bay and Cramond (locations 8 and 9) and nearby at South Queensferry (Saad and Wade, 2016) on the east coast of Scotland, and at Dunstaffnage and Loch Sunart (locations 4 and 6) on the west coast, at similar latitudes. However further north, differences between the biogeographic provinces were observed. On the east coast in the cool Boreal province only a single specimen was identified at Cromarty (location 2; 57°N), whilst on the west coast, in the warmer Boreal-Lusitanean province, *Ammonia* was commonly found further north at North Uist (location 3; 57°N), where 29 intertidal *Ammonia* were genotyped. *Ammonia* was also observed in Shetland but in subtidal populations only. No intertidal specimens were observed in any of the intertidal mud and seaweeds sampled here. On a northerly transect, therefore, the intertidal *Ammonia* populations decrease prior to the subtidal ones. This makes ecological sense, as the intertidal assemblage would be exposed to greater temperature fluctuations and hence lower temperatures in winter than assemblages in the subtidal zone. The Shetland-Orkney channel also represents a weak eastern boundary between the Boreal-Lusitanean, and the Boreal provinces, and although Shetland sits in the Boreal province, some species here are “southern” species and are not found in other locations in the boreal North Sea (Dinter, 2001).

4.5 Distribution and ecology of **Ammonia** *genetic types in the NE Atlantic*

The seven genetic types and subtypes identified in the NE Atlantic margins have both regional and potentially local ecological distinction. This is manifest in differences between the genetic types in their biogeography, depth preferences, or propensity to co-occur. Such information can be used to contribute to our understanding of the possibility of finding a specific *Ammonia* genetic type at a given location, even though they may be morphologically cryptic. The differences in their biogeography are presented in Figs. 7 and 8. The variations in biogeography and habitat and co-occurrences are summarized in Tables 6 and 7.

4.5.1 Biogeography and ecology of individual genetic types

Genetic type T1. – Although rare in our dataset (only eight T1 specimens were identified across four sampling locations (Fig. 7a) in our study) collated data indicate that the T1 genetic type has a broad distribution (Saad and Wade, 2016; Tables S1 and S5). It was found throughout the NE Atlantic margins in a range of biogeographic provinces (the Skagerrak subprovince and the Boreal, Boreal-Lusitanean and Lusitanean-Boreal provinces) and the western Mediterranean Sea (Fig. 7a). T1 has been collected from environments ranging from fully marine intertidal mudflats including estuarine systems to brackish high salt marsh environments (Table 6; Saad and Wade, 2016). It was also identified at subtidal depths (30 m) in low numbers in fjord environments off the west coast of Scotland (Table 1). In our dataset, T1 tended to be the least numerous in mixed *Ammonia* assemblages. However, Saad and Wade (2016) found that T1 dominated at two sites on the west coast of the UK within the cool Boreal province of the Irish Sea, but it was not found in the North Sea Boreal province, north of Norfolk (location 13; Figs.1 and 7). This, together with its presence further south in the warmer Lusitanean-Boreal province (Holzmann and Pawlowski, 1997) the Mediterranean (Holzmann and Pawlowski, 1997; Pawlowski et al. 1995; 1997) and sub-tropical locations (Hayward et al., 2004) indicate that it tends to prefer relatively warmer waters. It is associated with soft deep muddy sediments and muddy sand sediments (Table 6). T1 is predominantly an intertidal genetic type but has been found subtidally at two sites.

Genetic subtype T2A. – The T2A genetic subtype is a common member of the *Ammonia* assemblage in the Boreal-Lusitanean province and the Boreal provincial regions of the east and south coasts of England (Fig. 7b; Saad and Wade, 2016). However, only a single T2A specimen was found in the *Ammonia* assemblages further north in the western North Sea (location 2, Fig. 1; Table 1). Neither was it found in the Boreal provincial coastal waters of the eastern North Sea, in the West Norwegian subprovince off Scandinavia or in the Skagerrak subprovince. This implies that T2A is largely associated with the relatively warmer waters of the Boreal-Lusitanean province and its presence in the southwestern North Sea may

be due to the possible encroachment of the Boreal-Lusitanean provincial conditions into the southern North Sea in response to global climate change. Its preference for warmer water is consistent with its presence further south in the warmer Lusitanean-Boreal province (Holzmann and Pawlowski, 1997, 2000) and the Mediterranean (Pawlowski et al., 1995; 1997). T2A was collected from soft muddy intertidal sediments and estuarine environments (Table 1). A transect study of the steep shoreline at Dartmouth (location 18; Fig. 9) indicates that T2A is able to survive higher up the shore than the other *Ammonia* genetic types in the intertidal assemblage, suggesting that it has a high tolerance to temperature and salinity extremes. This finding is supported by the study of Saad and Wade (2016), who reported that T2A was found in sandy mud in a high salt marsh habitat, not routinely covered by seawater at every high tide. It was never found subtidally and is therefore an intertidal specialist.

Genetic subtype T2B. – T2B has the most southerly distributed biogeography of all the genetic types identified in the NE Atlantic margins (Fig. 7c). It is the only genetic type (other than the highly restricted T3V) that has not yet been identified in the Boreal province. Its most northerly distribution is around Cork (location 16) and on the Welsh south coast (Saad and Wade 2016), both located in the southern part of the Boreal-Lusitanean province. T2B alone was found at the most southerly sampling location in this study, the Guadiana River (location 22). It has also been found in the Lusitanean-Boreal province and in the Mediterranean Sea (Tables S1 and S5). T2B appears to have a requirement for slightly warmer waters than all the other genetic types identified in the region. Yet, similarly to other partially cryptic types, its habitat preference is still to inhabit intertidal mudflats in estuarine systems composed of soft muddy sediments or hard muddy sand (Table 6; Saad and Wade, 2016).

Genetic subtype T3S. – T3S has the widest biogeographical range of all genetic types identified in this study. It is the most northerly genetic type (Shetland, location 1), and it was identified in nine sampling locations in this study (in the Boreal and Boreal-Lusitanean provinces, the Cool Lusitanean subprovince and the Mediterranean; Fig. 8a). It was also identified in the Skagerrak subprovince (Holzmann and Pawlowski, 2000; Table S1) and the Lusitanean-Boreal province (Ertan et al., 2004). Not only is T3S found in a wide range of biogeographical provinces, it is also found in diverse habitats (Tables 1 and 6) from intertidal seaweeds (location 3) and mud (location 2), intertidal estuarine mud (location 18), and subtidal sediments (locations 1, 4, 5, 6, 21 and 22). T3S, therefore, should be regarded as a highly adaptable generalist species in European waters.

A transect study of the steep shoreline at Dartmouth (location 18), where three genetic types (T1, T2A and T3S) were identified, highlights the differences in their habitat preferences (see section 4.5.2). T3S was found at both low- and mid-shore sites, though numbers were lower in the mid-shore samples. It was completely absent from the upper shore. The drop off in numbers up-shore fits with our understanding that T3S is both an intertidal and subtidal genetic type, also found in the deepest sites where *Ammonia* was identified in this study.

Genetic subtype T3V. – Particularly interesting is that this genetic subtype is highly localised to the region of Vendée, on the French Atlantic coast (Fig. 8b; Pawlowski et al., 1995; Ertan et al., 2004; Hayward et al., 2004; this study). We collected T3V from intertidal seaweeds on Ile d'Yeu (location 19) off the Vendée coast. All specimens reported in the literature were from intertidal habitats, but whether from sediments or seaweeds is unknown.

Genetic type T6. – This is the only genetic type that has been widely reported in the Boreal province of the North Sea (Fig. 7d), where *Ammonia* is considered ubiquitous. T6 may therefore account for the majority of the *Ammonia* specimens sampled from this region. It is also found in the Boreal province of the Irish Sea (Saad and Wade 2016), and to a lesser extent in the Boreal-Lusitanean province, where it is found on the Welsh south coast (locations 14 and 17) bordering the Boreal province. It was not found further south in the Boreal-Luistanean province at either Cork (location 16) or Dartmouth (location 18) in this study. We did, however, identify two T6 specimens further south at Baie de l'Aiguillon in the Lusitanean-Boreal province. We did not find T6 further south in the Portuguese margin (location 22) or the Rhône prodelta (location 21) in the Mediterranean, but these fully marine subtidal habitats are not preferred by T6. However, despite a range of intertidal sampling in the Gulf of Lions (at Camargue, Le Boucanet and Banyuls-sur-Mer; see Tables S1 and S5) and in the Adriatic Sea (Trieste, Lagoon of Venice; Tables S1 and S5) this genetic type has not been reported there to date.

We have found T6 widely in brackish environments on the intertidal and estuarine shores within our study area and at one subtidal site of low salinity (location 7). This supports the finding of Schweizer et al. (2011b), who identified T6 subtidally (between 4-14 m) in the Kiel Fjord, in a lens of low salinity Baltic seawater. Such salinities may be more akin to the intertidal and estuarine environments, in which T6 has thus far has been found. Contrary to this, T6 was also found in the saline Grevelingen Lake (location 15) in The Netherlands. The lake was part of the Rhine River delta prior to being dammed, with a later edition of a sluice gate resulting in salinities of 29-32 (Hagens et al., 2015). T6 may be an invading species via the sluice, as it is widely distributed along the coast here. Cores from Grevelingen show that

prior to damming, the *Ammonia* specimens present had smaller pores, suggesting the presence of T2A rather than T6. After the closure of the lake, there was a shift to specimens with larger pores, suggesting an invasion of the lake by T6 via the sluice gate (Petersen et al., 2016). Its presence at these marine salinities, would indicate that it is a euryhaline species, despite a probable preference for brackish environments. Saad and Wade (2016) found *Ammonia* T6 around the UK in 14 of 19 sites sampled, and all but one of these 14 sites were described as brackish. The final sampling site, where T6 was identified however (Barrow-in-Furness; on the English west coast in the Boreal province), was described by these authors as fully marine. However, no salinity measurements were reported for any of the sampling sites and certainly, the majority of sites where T6 has been found are intertidal and estuarine mudflats, which will experience fluctuating salinities.

Genetic type T15. – T15 is relatively rare in our dataset. However, it was identified along the NE Atlantic margins where *Ammonia* is found at subtidal locations in the Boreal and Boreal-Lusitanean provinces, the Cool-Lusitanean subprovince and the Mediterranean (Fig. 8c). The only other molecular data available for this genetic type identified T15 in the Mediterranean Sea (Rhône prodelta) and the Bay of Biscay in accordance with previous morphologically based studies which also found this type in the Adriatic Sea (Schweizer et al., 2011a and references therein). Subtidal sampling off Shetland yielded no T15 specimens, whilst T3S was identified here. This may be either due to the presence of cooler waters, or the requirement for more extensive regional sampling. It is important to note that T15 is a fully marine species, restricted to subtidal muddy organic matter rich habitats.

4.5.2 Co-occurrence of **Ammonia** *genetic types*

It is of great importance for accurate data interpretation, to know whether more than one *Ammonia* genetic type is present, at any given sampling site. Of the 22 locations in this study, 13 locations contained only one genetic type, six locations contained two genetic types and three locations contained three genetic types. Their degree of co-occurrence is documented in Tables 6 and 7. Of significance is the fact that the smaller, less ornate cryptic genetic types T1, T2A, T2B and T6 co-occur in a variety of combinations (T1+T2A, T2A+T6, T1+T2B). In addition, T3S also co-occurs with T1 and T2A intertidally, as well as T1 and T15 subtidally. In agreement with our data from Cork, GenBank sequences (Supplementary Table S5) also place genetic types T1 and T2B together in Trieste in Italy, and with T2A in the Gulf of Lions (Camargue, French Mediterranean coast) and in the Lagoon of Venice, Italy (Holzmann et al., 1996; Pawlowski et al., 1997; Holzmann and Pawlowski, 2000). It is noteworthy that, despite T3S and T6 being relatively abundant and found at nine separate locations each, they were

never identified together (Table 7). This is most likely due to their differing ecological preferences, but this requires further sampling for confirmation.

The presence of different combinations of genetic types at different locations along a single shore transect at Dartmouth highlights the importance of clarifying the exact location of sampling on the intertidal shore (Fig. 9). For example, where T2A has been identified alone (e.g., locations 2 and 11, this study; Lymington: Saad and Wade, 2016), it is possible that only the upper shore was sampled, and that sampling the lower shore might reveal co-occurrence with other genetic types. We therefore recommend sampling at different heights on the shoreline, or to record the height at which samples are taken.

Of particular interest is that T6 very rarely co-occurred with the other genetic types in this study. Indeed, we identified only one example (a single specimen of T2A co-occurring with T6 at Norfolk; location 13; Table 7). Also, of the 14 sampling locations in the UK investigated by Saad and Wade (2016) where T6 was identified, T6 inhabited eleven sites alone and co-occurred with a second genetic type at only three sites, all in the Boreal province. In continental Europe, T6 was found alone in the Boreal province on the German coastline at Wilhelmshaven (Holzmann and Pawlowski, 2000), Crildumersiel (Langer and Leppig, 2000) and Amrum (Ertan et al., 2004) and on the coast of The Netherlands at Den Oever (Schweizer et al., 2011b). However, it was also found with T1 in The Netherlands at a single location, Mok Baai, (Holzmann and Pawlowski, 2000). In total, T6 has been reported at 29 locations in the NE Atlantic margins, but only co-occurred at five. This indicates that it may be a highly robust genetic type, able to out-compete others when salinity and other conditions favour it.

4.6 Global biogeographical patterns of the NE Atlantic **Ammonia** *genetic types*

Outside Europe, T1 genetic types were identified in Australia, New Zealand, New Caledonia, Chile, Cuba, and the USA east coast (Supplementary Tables S1 and S5), demonstrating the cosmopolitan nature of this genetic type, despite the low numbers we observed in the NE Atlantic margins. On the other hand, a single GenBank LSU sequence originating from Cape Cod in the USA (Supplementary Table S5) identified T2A as potentially confined to the Atlantic, as it has yet to be identified in the Pacific or Indian Oceans. T3S has not been reported outside Europe (Hayward et al., 2004). However, in this study, T3S was found subtidally at six out of the nine sampling locations where it was identified. If global sampling was largely confined to intertidal margins, it may have been missed, as in the intertidal study around the British Isles by Saad and Wade, (2016). However, several potential endemic

Ammonia genetic types have been identified in other regions globally (Hayward et al, 2004), suggesting that T3S could equally be endemic to the NE Atlantic. This possibility is confirmed by the extreme endemism exhibited by its sister genetic type T3V, which appears isolated within a small coastal region of France in the NE Atlantic. The genetic type T6 has only been found in Europe, Japan and China to date (Holzmann and Pawlowski, 2000; Hayward et al., 2004; Schweizer et al., 2011b) (Tables S1 and S5; Fig.7c), and this disjunct distribution may indicate a possible exotic species (discussed below). T2B, originally designated as part of the T2 cluster by Hayward et al. (2004; Fig. 3), has yet to be identified outside European waters (Hayward et al., 2004) again implying that it may be endemic to NE Atlantic margins and the Mediterranean. Finally, T15 has not been documented from other regions, but this may be due to its subtidal nature and the predominance of intertidal sampling globally as mentioned above.

There are a number of genetic types found in other regions that have not been identified in the NE Atlantic margins. For example, genetic types T7 and T9 are found on the east coast of the USA in temperate waters, but unlike T1 and T2A that are also found in the NE Atlantic, they are not transatlantic genetic types. The reasons for the differences in the biogeography of these genetic types is not yet clear, but may be a function of their ecology and the NE Atlantic circulation. T11 is found in the Caribbean and Cuba but has not been found further north on the USA coastline. T11 has not been found in the NE Atlantic margins and is most likely a warmer water specialist. This is in direct comparison to the ubiquitous T1, which although found in warm Cuban waters, is also a transatlantic genetic type able to tolerate wide temperature gradients.

4.7 Potential expatriation of T6

The disjunct distribution of T6 in the North Sea, China and Japan observed by Hayward et al (2004) led to the hypothesis that it originally came from Asia through ship ballast water to the North Sea (Pawlowski and Holzmann, 2008). Evidence for this came from the congruent distribution in Asia of *Ammonia* sp. T6 with the decapod *Eriocheir sinensis,* which was introduced to the Wadden Sea at the end of the 19th century via shipping (Nehring and Leuchs, 2000). In the present study, and that of Saad and Wade (2016), it has been shown that the distribution of T6 is far broader in Europe than previously recorded (Fig.7d). There are two possible inferences from this. Firstly, increased sampling of its favoured estuarine mudflat habitats might reveal a non-disjunct distribution, with a more global dispersal for T6 than currently recognised. For example, T6 has been found far up in to the Forth River system at both Torry Bay (location 8) and Cramond (location 9). Secondly, the observed wider

distribution in Europe might infer that invasion via ballast has led to extremely rapid colonisation of a wide area (including the UK west coast; Saad and Wade, 2016), due to its adaptable euryhaline nature. T6 may be an aggressive invasive species, able to outcompete indigenous genetic types. Down-core sampling to check the presence of T6 in Europe in the past decades or centuries would be of benefit. However, the morphological identification of T6 and its discrimination from other genetic types (T1, T2A and T2B) would be required (see Richirt et al., in press).

Core data from the outer Kiel Fjord demonstrates the late arrival (2000) of *Ammonia* to the area. This coincided with a decrease in salinity that favoured invasion of the fjord by *Ammonia* and excluded the strong-halocline adapted *Ammotium cassis* that previously made up to 90% of the foraminiferal abundance (Polovodova et al., 2009). Genetic characterisation of the *Ammonia* genetic types in the Kiel Fjord identified them as T6 (Schweizer et al., 2011b). Although *Ammonia* was thought to be absent from the Baltic Sea under the present salinity conditions (Hermelin, 1987; Murray, 2006: p. 66), we have demonstrated the presence of T6 also in Hanö Bay (location 7), with a population that could have been seeded by propagules from the Kiel Fjord, and the Kattegat and Skagerrak Seas (see Fig. 7d). The question remains as to the original source of *Ammonia* sp. T6 to the area. It is not known whether it is a globally distributed genetic type, that has slowly moved into the Kattegat and Baltic Seas as conditions have become more favourable to it, or if it is indigenous to China and Japan, transported in ballast water to the North Sea area and rapidly colonising the region, or vice versa. Only further global sampling of the brackish environments that it prefers will provide clues to its full biogeography.

5 Summary and conclusions

This study represents the first major genetic, biogeographic and morphometric investigation carried out on *Ammonia* specimens within the NE Atlantic margins. Here, *Ammonia* comprises seven genetic types and subtypes (T1, T2A, T2B, T3S, T3V, T6 and T15). Phylogenetic analyses were unable to resolve the relationships between the subtypes T2A and T2B or T3S and T3V and a focussed genetic survey of their intra-individual SSU variants is required to establish their genetic distinction and biogeography. The nomenclature for classifying the degree of genetic separation within and between benthic foraminiferal morphospecies and genera such as *Ammonia* are in serious need of stability and clarification. Morard et al., (2016), have proposed a nomenclature for use in planktonic foraminifera that can be applied to prescribed levels of divergence. We would argue for its adoption for benthic

foraminifera, as it would provide a framework for characterising and the naming the different levels of genetic divergence we observe.

This study has demonstrated that ecological niches can be used to help discriminate between *Ammonia* genetic types within the NE Atlantic margins. Subtidal *Ammonia* specimens will either be the morphologically distinguishable genetic types T3S (*A. batava*) or T15 (*A. falsobeccarii*). In fully marine subtidal regions, T1 may also be present, which is distinguishable from both T3S and T15. However, in more brackish subtidal waters, T1, T3S and T15 will not be present, and *Ammonia* specimens here are likely to be T6. Intertidal specimens are more difficult to delineate, particularly since co-occurrence of two to three types is common. However, the proportionate composition of upper slope genetic types differs from that of the lower slope ones, and this knowledge together with the biogeographical distribution of the different types contributes significant information towards the enhancement of (palaeo)ecological regional studies. This demonstrates the importance and value of identifying *Ammonia* at the biological species level instead of lumping them as cosmopolitan morphotypes, which provides limited environmental information.

Acknowledgements

We thank Jung-Hyun Kim and the crew of the R/V *Pelagia* (NIOZ) for the PACEMAKER cruise off the Portuguese coast, the crews of the R/V *Tethys II* (CNRS-INSU) for the sampling in the Rhône prodelta. The samples from the Baltic Sea were collected within the project "Field and culture-based calibration of temperature and salinity proxies using benthic foraminifera" funded by the Swedish Research Council (grants no 621-2011-5090) and we thank the crew and the captain of R/V *Skagerak*. We also want to thank people who have collected or isolated samples: Linda Kirstein, Julia Docherty (University of Edinburgh); Nikki Khanna, David McCarthy, Heather Austin (University of St Andrews), Anne Bevan (University of the Highlands and Islands); Jeroen Groeneveld (University of Bremen); Michael and Susan Edwards (Dartmouth, UK); RSPB Orkney; Dario Ledda (Geneva, Switzerland); Dewi Langlet, Eric Bénéteau, Christine Barras and Frans Jorissen (University of Angers, France); Filip Meysman (NIOZ, Netherlands); Isabel Mendes (University of Algarve, Portugal). Thanks also go to Gillian McKay for invaluable help with figures.

This work was funded by the Natural Environment Research Council (NERC) of the United Kingdom (grant NE/G020310/1 to K.D., W.E.N.A. and M.S.) and the Carnegie Trust for the Universities of Scotland. M.S. was supported by the Swiss National Science Foundation (SNSF, fellowships for advanced researchers PA00P2_126226 and PA00P2_142065).

References

Alve, E., Goldstein, S., 2003. Propagule transport as a key method of dispersal in benthic foraminifera (Protista). Limnol. Oceanogr. 48, 2163–2170. Doi: 10.4319/lo.2003.48.6.2163

Alve, E., and Nagy, J., 1990. Main features of foraminiferal distribution reflecting estuarine hydrography in Oslo Fjord. Mar. Micropaleontol.16.3-4: 181-206. Doi: 10.1016/0377-8398(90)90003-5

Alve, E., Murray, J., 1999. Marginal marine environments of the Skagerrak and Kattegat: a baseline study of living (stained) benthic foraminiferal ecology. Palaeogeogr. Palaeoclim. Palaeoecol. 146, 171–193. Doi: 10.1016/S0031-0182(98)00131-X

Asano, K., 1951. Illustrated catalogue of Japanese Tertiary smaller foraminifera Part 14: Rotaliidae.

Austin,W.E.N., Sejrup, H.P., 1994. Recent shallow water benthic foraminifera from Western Norway: Ecology and Palaeoecological Significance. vol. 32. Cushman Foundation for Foraminiferal Research, Special Publication 39, 103–125.

Bergsten, H. 1996. Recent benthic foraminifera as tracers of water masses along a transect in the Skagerrak, north-eastern North Sea. Neth J Sea Res 35, 111–121. Doi: 10.1016/S1385-1101(96)90740-6

Boltovskoy, E., Wright, R., 1976, Recent Foraminifera. Junk Publishers, The Hague, 515.

Conradsen, K., 1993. Recent benthic foraminifera in the southern Kattegat, Scandinavia: distributional pattern and controlling parameters. Boreas. 22, 367-382. Doi: 10.1111/j.1502-3885.1993.tb00200.x

Conradsen, K., Bergsten, H., Knudsen, K.L., Nordberg, K. & Seidenkrantz, M.-S., 1994. Recent foraminiferal distribution in the Kattegat and the Skagerrak, Scandinavia. Cushman Foundation for Foraminiferal Research, Special Publication 32, 53-68. Doi: 10.1111/j.1502-3885.1993.tb00200.x

Corner, G., Steinsund, P., Aspeli, R., 1996. Distribution of recent benthic foraminifera in a subarctic fjord-delta: Tana, Norway. Mar. Geol. 134, 113–125. Doi: 10.1016/0025-3227(96)00039-4

Cushman, J.A., 1926. Recent foraminifera from Porto Rico. Publications of the Carnegie Institution of Washington, 342, 73-84.

De Nooijer L. J., Langer, G., Nehrke G., and Bijma J., 2009. Physiological controls on seawater uptake and calcification in the benthic foraminifer *Ammonia tepida*. Biogeosciences 6, 2669-2675. Doi: 10.5194/bg-6-2669-2009

Dutton, A., Carlson, A.E., Long, A.J., Milne, G.A., Clark, P.U., DeConto, R., Horton, B.P., Rahmstorf, S., Raymo, M.E., 2015. Sea-level rise due to polar ice-sheet mass loss during past warm periods. Science. 349, aaa4019. Doi: 10.1126/science.aaa4019

Darling, K., Schweizer, M., Knudsen, K., Evans, K., Bird, C., Roberts, A., Filipsson, H., Kim, J.-H., Gudmundsson, G., Wade, C., Sayer, M., Austin, W., 2016. The genetic diversity, phylogeography and morphology of Elphidiidae (Foraminifera) in the Northeast Atlantic. Mar. Micropaleontol. 129, 1–23. Doi: 10.1016/j.marmicro.2016.09.001

Dinter, W.P., 2001. Biogeography of the OSPAR maritime area. A synopsis and synthesis of biogeographical distribution patterns described for the North-east Atlantic. Federal Agency for Nature Conservation, Bonn, Germany (167 pp.).

Dissard, D., Nehrke, G., Reichart, G.J., Bijma, J., 2010. Impact of seawater pCO_2 on calcification and Mg/Ca and Sr/Ca ratios in benthic foraminifera calcite: results from culturing experiments with *Ammonia tepida*. Biogeosciences 7, 81–93. Doi: 10.5194/bg-7-81-2010

Elderfield, H., Yu, J.M., Anand, P., Kiefer, T., Nyland, B., 2006. Calibrations for benthic foraminiferal Mg/Ca paleothermometry and the carbonate ion hypothesis. Earth Planet. Sci. Lett. 250, 633-649. Doi: 10.1016/j.epsl.2006.07.041

Ellis, B.F.S., and Messina A.R., 1940 and supplements. Catalogue of foraminifera. New York. American Museum of Natural History, Micropaleontology Press.

Ertan, K.T., Hemleben, V., Hemleben, C., 2004. Molecular evolution of some selected benthic foraminifera as inferred from sequences of the small subunit ribosomal DNA. Mar. Micropaleontol. 53, 367–388. Doi: 10.1016/j.marmicro.2004.08.001

Felsenstein, J., 1985. Phylogenies and the Comparative Method. The American Naturalist 125, 1-15. https://www.jstor.org/stable/2461605

Foster, W.J., Armynot du Châtelet, E., Rogerson, M., 2012. Testing benthic foraminiferal distributions as a contemporary quantitative approach to

biomonitoring estuarine heavy metal pollution. Mar. Pollut. Bull. 64, 1039–48. Doi: 0.1016/j.marpolbul.2012.01.021

Frontalini, F., and Coccioni, R., 2008. Benthic foraminifera for heavy metal pollution monitoring: A case study from the central Adriatic Sea coast of Italy. Estuar Coast Shelf Sci 76, 404–417. Doi: 10.1016/j.ecss.2007.07.024

Frontalini, F., Curzi, D., Giordano, F.M., Bernhard, J., Falcieri, E., Coccioni, R., 2015. Effects of Lead Pollution on Ammonia Parkinsoniana (Foraminifera): Ultrastructural and Microanalytical Approaches. Eur J Histochem. 59, 2469. Doi:10.4081/ejh.2015.2460.

Garcia-Vallvé, S., Palau, J., Romeu, A. 1999. Horizontal gene transfer in glycosyl hydrolases inferred from codon usage in *Escherichia coli* and *Bacillus subtilis*. Mol. Biol. Evol. 16, 1125-1134. Doi: 10.1093/oxfordjournals.molbev.a026203

Gascuel, O., 1997. BIONJ: an improved version of the NJ algorithm based on a simple model of sequence data. Mol. Biol. Evol. 14, 685-695. Doi: 10.1093/oxfordjournals.molbev.a025808

Gehrels, R., Kirby, J., Prokoph, A., Newnham, R., Achterberg, E., Evans, H., Black, S., Scott, D., 2005. Onset of recent rapid sea-level rise in the western Atlantic Ocean. Quat Sci Rev 24, 2083–2100. Doi: 10.1016/j.quascirev.2004.11.016

Glock, N., Eisenhauer, A., Milker, Y., Liebetrau, V., Schönfeld, J., Mallon, J., Sommer, S., Hensen, C., 2011. Environmental influences on the pore density of Bolivina spissa (Cushman). J. Foraminifer Res. 41, 22–32. Doi: 10.2113/gsjfr.41.1.22

Gouy, M., Guindon, S., Gascuel, O., 2010. SeaView Version 4: A Multiplatform Graphical User Interface for Sequence Alignment and Phylogenetic Tree Building. Mol. Biol. Evol. 27, 221–224. Doi: 10.1093/molbev/msp259

Groeneveld, J., Filipsson, H.L., 2013. Mg/Ca and Mn/Ca ratios in benthic foraminifera: the potential to reconstruct past variations in temperature and hypoxia in shelf regions. Biogeosciences. 10, 5125-5138. Doi: 10.5194/bg-10-5125-2013

Groeneveld, J., Filipsson, H.L., Austin, W.E.N., Darling, K.F., McCarthy, D., Nadine B. Quintana Krupinski, N.B., Bird, C., Schweizer, M., 2018. Assessing proxy signatures of temperature, salinity and hypoxia in the Baltic Sea through

foraminifera-based geochemistry and faunal assemblages. J Micropalaeontol 37, 403-429. Doi: 10.5194/jm-37-403-2018

Guillou, L., Bachar, D., Audic, S., Bass, D., Berney, C., Bittner, L., Boutte, C., Burgaud, G., de Vargas, C., Decelle, J., Campo, J. del, Dolan, J., Dunthorn, M., Edvardsen, B., Holzmann, M., Kooistra, W., Lara, E., Bescot, N., Logares, R., Mahé, F., Massana, R., Montresor, M., Morard, R., Not, F., Pawlowski, J., Probert, I., Sauvadet, A.-L., Siano, R., Stoeck, T., Vaulot, D., Zimmermann, P., Christen, R., 2013. The Protist Ribosomal Reference database (PR2): a catalog of unicellular eukaryote Small Sub-Unit rRNA sequences with curated taxonomy. Nucleic Acids Res. 41, D597–D604. Doi: 10.1093/nar/gks1160

Guindon, S., Gascuel, O., Rannala, B., 2003. A Simple, Fast, and Accurate Algorithm to Estimate Large Phylogenies by Maximum Likelihood. Syst. Biol. 52, 696–704. Doi: 10.1080/10635150390235520

Hagens, M., Slomp, C.P., Meysman, F.J.R., Seitaj, D., Harlay, J., Borges, A.V., Middelburg, J.J., 2015. Biogeochemical processes and buffering capacity concurrently affect acidification in a seasonally hypoxic coastal marine basin. Biogeosciences. 12, 1561–1583. Doi: 10.5194/bg-12-1561-2015

Hall, T.A., 1999. BioEdit: a user-friendly biological sequence alignment editor and alignment analysis program for Windows 95/98/NT. Nucleic Acid Symp. Ser. 41, 95-98.

Hammer, Ø., Harper, D.A.T., Ryan, P.D., 2001. PAST: Paleontological statistics software package for education and data analysis. Palaeontol Electronica. 4, 9pp. https://palaeo-electronica.org/2001_1/past/past.pdf

Hasegawa, M., Kishino, H., Yano, T., 1985. Dating of the human-ape splitting by a molecular clock of mitochondrial DNA. J. Mol. Evol. 22, 160–174. Doi: 10.1007/bf02101694

Haynert, K., Schönfeld, J., Polovodova-Asteman, I., Thomsen, J., 2012. The benthic foraminiferal community in a naturally CO_2-rich coastal habitat of the southwestern Baltic Sea. Biogeosciences. 9, 4421–4440. Doi: 10.5194/bg-9-4421-2012

Haynes, J.R., 1973. Cardigan Bay Recent Foraminifera. Bulletin of the British Museum of Natural History (Zoology). 4, 1-145

Haynes, J.R., 1992. Supposed pronounced ecophenotypy in foraminifera. J Micropalaeontol 11, 59–63. Doi: 10.1144/jm.11.1.59

Hayward, B., Buzas, M.A., Buzas-Stephens, P., Holzmann, M., 2003. The lost types of *Rotalia beccarii* var. *tepida* Cushman 1926. J Foramin Res. 33, 352-354.

Hayward, B., Holzmann, M., Grenfell, H., Pawlowski, J., Triggs, C., 2004. Morphological distinction of molecular types in Ammonia – towards a taxonomic revision of the world's most commonly misidentified foraminifera. Mar. Micropaleontol. 50, 237–271. Doi: 10.1016/S0377-8398(03)00074-4

Healey, S. L., Thunell, R.C., Corliss, B.H., 2008. The Mg/Ca-temperature relationship of benthic foraminiferal calcite: New core-top calibrations in the <4°C temperature range. Earth Planet. Sci. Lett. 272, 523-530. Doi: 10.1016/j.epsl.2008.05.023

Hermelin, J.O.R., 1987. Distribution of Holocene benthic foraminifera in the Baltic Sea. J. Foraminifer Res. 17, 62-73. Doi: 10.2113/gsjfr.17.1.62

Hiscock, K., and Breckels, M., 2007. Marine biodiversity hotspots in the UK: their identification and protection. Godalming: WWF-UK. Marine Biological Association Report. Plymouth.

Hofker, J., 1951. The foraminifera of the Siboga expedition; part III. Siboga Exped. Monogr., Leiden, 4b:498-502

Holzmann, M., 2000. Species Concept in Foraminifera: *Ammonia* as a Case Study. Micropaleontology 46, 21-37. https://www.jstor.org/stable/1486178

Holzmann, M., Pawlowski, J., 1997. Molecular, morphological and ecological evidence for species recognition in *Ammonia* (Foraminifera). J Foraminifer Res. 27, 311–318. Doi: 10.2113/gsjfr.27.4.311

Holzmann, M., Pawlowski, J., 2000. Taxonomic relationships in the genus *Ammonia* (Foraminifera) based on ribosomal DNA sequences. J Micropalaeontol 19, 85–95. Doi: 10.1144/jm.19.1.85

Holzmann, M., Piller, W., Pawlowski, J., 1996. Sequence variations in the large-subunit ribosomal RNA gene of *Ammonia* (foraminifera, protozoa) and their evolutionary implications. J. Mol. Evol. 43, 145–151. Doi: 10.1007/bf02337359

Horton, B.P., Edwards, R.J., 2006. Quantifying Holocene Sea Level Change Using Intertidal Foraminifera: Lessons from the British Isles. Cushman Foundation for Foraminiferal Research, Special Publication 40. Retrieved from http://repository.upenn.edu/ees_papers/50

Huelsenbeck, J., Rannala, B., Buckley, T., 2004. Frequentist Properties of Bayesian Posterior Probabilities of Phylogenetic Trees Under Simple and

Complex Substitution Models. Syst. Biol. 53, 904–913. Doi: 10.1080/10635150490522629

Husum, K., Hald, M., 2004. Modern foraminiferal distribution in the subarctic Malangen Fjord and adjoining shelf, northern Norway. J Foraminifer Res. 34, 34–48. Doi: 10.2113/0340034

Jennings, A. E., Weiner, N. J., Helgadóttir, G. and Andrews, J. T., 2004. Modern foraminiferal faunas of the southwestern to northern Iceland shelf: oceanographic and environmental controls. J. Foraminifer Res. 34, 180–207. Doi: 10.2113/34.3.180

Jorissen, F.J., 1988. Benthic foraminifera from the Adriatic Sea; principles of phenotypic variation. Utrecht Micropaleontological Bulletins 37, 7-139

Jorissen, F., Nardelli, M.P., Almogi-Labin, A., Barras, C., Bergamin, L., Bicchi, E., El kateb, A., Ferraro, L., McGann, M., Morigi, C., Romano, E., Sabbatini, A., Schweizer, M., Spezzaferri, S., 2018. Developing Foram_AMBI for biomonitoring in the Mediterranean: Species assignements to ecological categories. Marine Micropaleontology. 140,33-45. Doi: 10.1016/j/marmicro.2017.12.006

Keul, N., Langer, G., de Nooijer L.J., Bijma J., 2013. Effect of ocean acidification on the benthic foraminifera *Ammonia* sp. is caused by a decrease in carbonate ion concentration. Biogeosciences. 10, 6185-6198. Doi: 10.5194/bg-10-6185-2013

Kimura, M., 1980. A simple method for estimating evolutionary rates of base substitutions through comparative studies of nucleotide sequences. J. Mol. Evol. 16, 111–120. Doi: 10.1007/bf01731581

Koho, K.A., LeKieffre, C., Nomaki, H., Salonen, I., Geslin, E., Mabilleau, G., Jensen, L.H., Reichart, G.-J., 2018. Changes in ultrastructural features of the foraminifera Ammonia spp. in response to anoxic conditions: Field and laboratory observations. Mar. Micropaleontol. 138, 72–82. Doi: 10.1016/j.marmicro.2017.10.011

Korsun, S., Hald, M., Golikova, E., Yudina, A., Kuznetsov, I., Mikhailov, D., Knyazeva, O., 2014. Intertidal foraminiferal fauna and the distribution of Elphidiidae at Chupa Inlet, western White Sea. Mar. Biol. Res. 10, 153-166, Doi: 10.1080/17451000.2013.814786

Kuhnt, T., Schiebel, R., Schmiedl, G., Milker, Y., Mackensen, A., Friedrich, O., 2014. Automated and manual analyses of the pore density-to-oxygen

relationship in *Globobulimina turgida* (Bailey). J. Foramininifer Res. 44, 5–16. Doi: 10.2113/gsjfr.44.1.5

Langer, M.R., Leppig, U., 2000. Molecular phylogenetic status of *Ammonia catesbyana* (D'Orbigny, 1839), an intertidal foraminifer from the North Sea. Neues jarbuch fur Geologie und Palaontologie Monatsheft. 2000, 545-556. ISSN: 0028-3630

Langer, G., Sadekov, A., Thoms, S., Keul, N., Nehrke, G., Mewes, A., Greaves, M., Misra, S., Reichart, G-I., de Nooijer, L.J., Bijma, J., Elderfield, H., 2016. Sr partitioning in the benthic foraminifera *Ammonia aomoriensis* and *Amphistegina lessonii*. Chem. Geol. 440, 306-312. Doi: 10.1016/j.chemgeo.2016.07.018

Le Cadre, V., Debenay, J.-P., 2006. Morphological and cytological responses of Ammonia (foraminifera) to copper contamination: Implication for the use of foraminifera as bioindicators of pollution. Environ. Pollut. 143, 304–317. Doi: 10.1016/j.envpol.2005.11.033

Lecroq, B., Lejzerowicz, F., Bachar, D., Christen, R., Esling, P., Baerlocher, L., Østerås, M., Farinelli, L., Pawlowski, J., 2011. Ultra-deep sequencing of foraminiferal microbarcodes unveils hidden richness of early monothalamous lineages in deep-sea sediments. Proc. Natl. Acad. Sci. U.S.A. 108, 13177–82. Doi: 10.1073/pnas.1018426108

Lei, Y., Li, T., Nigam, R., Holzmann, M., Lyu, M., 2016. Environmental significance of morphological variations in the foraminifer Ammonia aomoriensis (Asano, 1951) and its molecular identification: A study from the Yellow Sea and East China Sea, PR China. Palaeogeogr. Palaeoclim. Palaeoecol. 483, 49–57. Doi: 10.1016/j.palaeo.2016.05.010

LeKieffre, C., Bernhard, J., Mabilleau, G., Filipsson, H., Meibom, A., Geslin, E., 2018. An overview of cellular ultrastructure in benthic foraminifera: New observations of rotalid species in the context of existing literature. Mar. Micropaleontol. 138, 12–32. Doi: 10.1016/j.marmicro.2017.10.005

Linné, C., 1758. Systemae naturae, edition 10 Stockholm, Sweden. Tomus 1, 710.

Loeblich, A. R. and Tappan, H. 1987. Foraminiferal Genera and their Classification. Van Nostrand Rienhold Co., New York.

Lutze, G. 1965. Zur Foraminiferen-Fauna der Ostsee. Meyniana. 15, 75-142.

Mitchell, R.,Earll, R.C., Dipper, F.A., 1983. Shallow sublittoral ecosystems in the Inner Hebrides. Proc Royal Soc Edinb Biol. 83, 161–183. Doi: 10.1017/S0269727000013397

Morard, R., Quillevere, F., Escarguel, G., Ujiie, Y., de Garidel-Thoron, T., Norris, R.D., de Vargas, C., 2009. Morphological recognition of cryptic species in the planktonic foraminifer *Orbulina universa*. Mar. Micrpaleontol. 71, 148-165. Doi: 10.1016/j.marmicro.2009.03.001

Morard, R., Darling, K., Mahé, F., Audic, S., Ujiié, Y., Weiner, A., André, A., Seears, H., Wade, C., Quillévéré, F., Douady, C., Escarguel, G., Garidel-Thoron, T., Siccha, M., Kucera, M., Vargas, C., 2015. PFR2: a curated database of planktonic foraminifera 18S ribosomal DNA as a resource for studies of plankton ecology, biogeography and evolution. Mol Ecol Resour. 15, 1472–1485. Doi: 10.1111/1755-0998.12410

Morard R, Escarguel G, Weiner AKM, André A, Douady CJ, Wade CM, Darling KF, Ujiié Y, Seears HA, Quillévéré F, de Garidel-Thoron T, de Vargas C, Kucera M., 2016. Nomenclature for the Nameless: A Proposal for an Integrative Molecular Taxonomy of Cryptic Diversity Exemplified by Planktonic Foraminifera. Systematic Biology 65, 925-940. Doi: 10.1093/sysbio/syw031

Murray, J.W., 1991. Ecology and palaeoecology of benthic foraminifera. Longman Scientific and Technical.

Murray, J.W., (ed) 2006. Ecology and Applications of Benthic Foraminifera. Cambridge University Press.

Murray, J., Alve, E., 2016. Benthic foraminiferal biogeography in NW European fjords: A baseline for assessing future change. Estuar Coast Shelf Sci. 181, 218–230. http://dx.doi.org/10.1016/j.ecss.2016.08.014

Nehring, S., Leuchs, H., 2000. Neozoen im Makrozoobenthos der Brackgewässer an der deutschen Nordseeküste. Lauterbornia. 39, 73-116.

Nehrke, G., Keul, N., Langer, G., de Nooijer, L.J., Bijma, J., Meibom, A., 2013. A new model for biomineralization and trace-element signatures of Foraminifera tests. Biogeosciences. 10, 6759–6767. Doi: 10.5194/bg-10-6759-2013

Nørvang, A. 1945. The Zoology of Iceland, Foraminifera 2 (2). E. Munksgaard, Copenhagen and Reykjavik, 79 pp.

Pawlowski, J., Bolivar, I., Farhni, J., Zaninetti, L., 1995. DNA analysis of "Ammonia beccarii" morphotypes: one or more species? Mar. Micropaleontol. 26, 171–178. Doi: 10.1016/0377-8398(95)00022-4

Pawlowski, J., Bolivar, I., Fahrni, J.F., Cavalier-Smith, T., Gouy, M., 1996. Early origin of foraminifera suggested by SSU rRNA gene sequences. Mol. Biol. Evol. 13, 445-450. Doi: 10.1093/oxfordjournals.molbev.a025605

Pawlowski J, Bolivar I, Fahrni JF, de Vargas C, Gouy M, Zaninetti L, 1997. Extreme differences in rates of molecular evolution of foraminifera revealed by comparison of ribosomal DNA sequences and the fossil record. Mol. Biol. Evol. 14, 498–505. Doi: 10.1093/oxfordjournals.molbev.a025786

Pawlowski, J., 2000. Introduction to the molecular systematics of foraminifera. Micropaleontology. 46, 1-12. https://www.jstor.org/stable/1486176

Pawlowski, J., Holzmann, M., 2008. Diversity and geographic distribution of benthic foraminifera: a molecular perspective. Biodivers. Conserv. 17, 317–328. Doi: 10.1007/s10531-007-9253-8

Pawlowski, J., Lecroq, B., 2010. Short rDNA barcodes for species identification in foraminifera. J. Eukaryot. Microbiol. 57, 197–205. Doi: 10.1111/j.1550-7408.2009.00468.x

Pawlowski, J., Audic, S., Adl, S., Bass, D., Belbahri, L., Berney, C., Bowser, S. S., Cepicka, I., Decelle, J., Dunthorn, M., Fiore- Donno, A. M., Gile, G. H., Holzmann, M., Jahn, R., Jirku° , M., Keeling, P. J., Kostka, M., Kudryavtsev, A., Lara, E., Lukesˇ, J., Mann, D. G., Mitchell, E. A. D., Nitsche, F., Romeralo, M., Saunders, G. W., Simpson, A. G. B., Smirnov, A. V., Spouge, J., Stern, R. F., Stoeck, T., Zimmermann, J., Schindel, D., and de Vargas, C., 2012. CBOL protist working group: barcoding eukaryotic richness beyond the animal, plant and fungal kingdoms. PLoS Biol. 10, p. e1001419. Doi: 10.1371/journal.pbio.1001419

Pawlowski, J., Holzmann, M., 2014. A plea for DNA barcoding of foraminifera. J. Foraminifer Res. 44, 62–67. Doi: 10.2113/gsjfr.44.1.62

Petersen, J., Riedel, B., Barras, C., Pays, O., Guihéneuf, A., Mabilleau, G., Schweizer, M., Meysman, F., Jorissen, F., 2016. Improved methodology for measuring pore patterns in the benthic foraminiferal genus Ammonia. Mar. Micropaleontol. 128, 1–13. Doi: 10.1016/j.marmicro.2016.08.001

Pillet, L., Fontaine, D., Pawlowski, J., 2012. Intra-Genomic Ribosomal RNA Polymorphism and Morphological Variation in Elphidium macellum Suggests

Inter-Specific Hybridization in Foraminifera. PloS ONE. 7, e32373. Doi: 10.1371/journal.pone.0032373

Polovodova, I., Nikulina, A., Schönfeld, J., Dullo, W.-C., 2009. Recent benthic foraminifera in the Flensburg Fjord (Western Baltic Sea). J Micropalaeontol. 28, 131–142. Doi: 10.1144/jm.28.2.131

Poole, D., Vorren, T., 1993. Miocene to Quaternary paleoenvironments and uplift history on the mid Norwegian shelf. Mar. Geol. 115, 173–205. Doi: 10.1016/0025-3227(93)90050-6

Quast C., Pruesse E., Yilmaz P., Gerken J., Schweer T., Yarza P., Peplies J., Glöckner F.O. 2013. The SILVA ribosomal RNA gene database project: improved data processing and web-based tools. Nucleic Acids Res. 41, D590-D596. Doi: 10.1093/nar/gks1219

Richirt, J., Schweizer, M., Bouchet, V. M. P., Mouret, A., Quinchard, S., Jorissen, F. J. In press. Morphological distinction of three *Ammonia* phylotypes occuring along the European coasts. Journal of Foraminiferal Research.

Risdal, D. 1964. The bathymetrical relation of Recent Foraminiferal Faunas in the Oslo Fjord, with a discussion of the Foraminiferal Zones from Late Quaternary time. Norges Geologiske Undersökelse 226, 1-142. (In Norwegian with English Summary).

Roberts, A., 2016. Reconciling molecules and morphology in benthic foraminifera: A morphometric study of *Ammonia* and Elphidiidae in the NE Atlantic. PhD Thesis. University of St Andrews.

Roberts, A., Austin, W., Evans, K., Bird, C., Schweizer, M., Darling, K., 2016. A New Integrated Approach to Taxonomy: The Fusion of Molecular and Morphological Systematics with Type Material in Benthic Foraminifera. PLoS ONE. 11, e0158754. Doi:10.1371/journal.pone.0158754

Ronquist, F., Teslenko, M., Mark, P. van der, Ayres, D., Darling, A., Höhna, S., Larget, B., Liu, L., Suchard, M., Huelsenbeck, J., 2012. MrBayes 3.2: Efficient Bayesian Phylogenetic Inference and Model Choice Across a Large Model Space. Syst. Biol. 61, 539–542. Doi: 10.1093/sysbio/sys029

Rosenthal, Y., Boyle, E.A., Slowey, N., 1997. Temperature control on the incorporation of magnesium, strontium, fluorine, and cadmium into benthic foraminiferal shells from Little Bahama Bank: Prospects for thermocline paleoceanography. Geochim. Cosmochim. Acta. 61, 3633-3643. Doi: 10.1016/S0016-7037(97)00181-6

Rouvillois, A., 1974. Un foraminifère méconnu du plateau continental du Golfe de Gascogne: *Pseudoeponides falsobeccarii*. Cahiers de Micropaléontologie. 1974, 3-5.

Saad, S., Wade, C., 2016. Biogeographic distribution and habitat association of Ammonia genetic variants around the coastline of Great Britain. Mar. Micropaleontol. 124, 54–62. Doi: 10.1016/j.marmicro.2016.01.004

Schnitker, D. 1974. Ecophenotypic variation in *Ammonia beccarii* (Linné). J. Foraminifer Res. 4, 216-223.

Schweizer, M., Pawlowski, J., Kouwenhoven, T. J., Guiard, J., Van Der Zwaan, G. J., 2008. Molecular phylogeny of the Rotaliida (Foraminifera) based on complete small subunit of rDNA sequences. Mar. Micropaleontol. 66: 233-246. Doi: 10.1016/j.marmicro.2007.10.003

Schweizer, M., Pawlowski, J., Kouwenhoven, T., van der Zwaan, B., 2009. Molecular phylogeny of common Cibicidids and related Rotaliida (foraminifera) based on small subunit rDNA sequences. J Foraminifer Res. 39, 300–315. Doi: 10.2113/gsjfr.39.4.300

Schweizer, M., Jorissen, F., Geslin, E., 2011a. Contributions of molecular phylogenetics to foraminiferal taxonomy: General overview and an example with *Pseudoeponides falsobeccarii* Rouvillois, 1974. C R Palevol. 10, 95-105. Doi: 10.1016/j.crpv.2011.01.003

Schweizer, M., Polovodova, I., Nikulina, A., Schönfeld, J., 2011b. Molecular identification of *Ammonia* and *Elphidium* species (Foraminifera, Rotaliida) from the Kiel Fjord (SW Baltic Sea) with rDNA sequences. Helgol Mar Res. 65, 1–10. Doi: 10.1007/s10152-010-0194-3

Schweizer, M., 2015. How long after death is DNA preserved *in situ* in intertidal foraminifera? J Micropalaeontol. 34, 217-219. Doi: 10.1144/jmpaleo2014-023

Sejrup, H.P., Birks, H.J.B., Klitgaard Kristensen, D., Madsen, H., 2004. Benthonic foraminiferal distributions and quantitative transfer functions for the northwest European continental margin. Mar. Micropaleontol. 53, 197–226. Doi: 10.1016/j.marmicro.2004.05.009

Tavaré S. 1986. Some probabilistic and statistical problems in the analysis of DNA sequences. In: Miura R.M, editor. Some mathematical questions in biology—DNA sequence analysis. American Mathematical Society; Providence, RI.

Toyofuku, M., Kitazato, H., Tsuchiya, M., 2005. Phylogenetic relationships among genus Ammonia (Foraminifera) based on ribosomal DNA sequences which are distributed in the vicinity of the Japanese Islands. Frontier Research on Earth Evolution 2.

Toyofuku, T., Matsuo, M.Y., de Nooijer, L.J., Nagai, Y., Kawada, S., Fujita, K., Reichart, G.-J., Nomaki, H., Tsuchiya, M., Sakaguchi, H., Kitazato, H., 2017. Proton pumping accompanies calcification in foraminifera. Nat Commun. 8, 14145. Doi: 10.1038/ncomms14145

Weber, A. A. T., & Pawlowski, J. 2014. Wide occurrence of SSU rDNA intragenomic polymorphism in Foraminifera and its implications for molecular species identification. Protist. 165, 645-661. Doi: 10.1016/j.protis.2014.07.006

Zachos, J., Pagani, M., Sloan, L., Thomas, E., Billups, K., 2001. Trends, Rhythms, and Aberrations in Global Climate 65 Ma to Present. Science. 292, 686–693. Doi: 10.1126/science.1059412

Figures

Fig. 1. Map of the NE Atlantic showing sampling locations in this study. Open circles (o) are locations where *Ammonia* was absent, and closed circles (●) are locations where *Ammonia* was successfully sequenced (numbered north to south, see Table 1). The map also shows the biogeographic classification of the benthic and neritopelagic regions of the shelf and upper continental slope (Dinter, 2001: Fig. 105).

Fig. 2. SEM image plate showing representative specimens typical of each *Ammonia* genetic type with umbilical and spiral sides. The apertural side is also presented for some individuals. Scale bar 100 µm.

Fig. 3. Molecular phylogeny of *Ammonia* based on partial SSU sequences inferred using the BioNJ method with the K2P model. The tree is unrooted and support values for BioNJ/ML-HKY+Γ/BA are indicated at the main nodes. Individual sequences are labelled with the SSU genetic types (S) where known and/or T-types (Hayward et al., 2004).

Fig. 4. UPGMA cluster dendrogram based on the morphological characteristics (Table 3) of the seven *Ammonia* genetic types across the NE Atlantic margins (n=158).

Fig. 5 Primary PCO analysis of the morphometric data of the seven distinct genetic types found in the NE Atlantic margins. Each group is bounded by a convex hull. The first two principle coordinates account for 35.6% of the total variation.

Fig.6. Secondary PCO analysis of the *Ammonia* morphometric data, excluding T3S and T3V, which were separated in the primary PCO analysis (Fig. 5). Each of the genetic types is bounded by a convex hull. The two principle components account for 28.8% of the total variation.

Fig. 7. Biogeographical distribution maps for the small less ornate, morphometrically overlapping genetic types; T1, T2A, T2B and T6. Biogeographic provinces where genetic types are located are shaded grey. Closed circles (●) represent specimens genetically identified in this study; open triangles (Δ) represent SSU sequences already in GenBank; and open squares (□) represent LSU sequences already in GenBank or specimens identified by restriction fragment length polymorphism (Denmark, T6 only).

Fig. 8. Biogeographical distribution maps of the morphologically identifiable genetic types T3S, T3V and T15. Biogeographic provinces where genetic types are located are shaded grey. Closed circles (●) represent specimens genetically identified in this study; open triangles (Δ) represent SSU sequences already in GenBank; and open squares (□) represent LSU sequences already in GenBank.

Fig. 9. Cross section of a shore transect taken at Dartmouth (UK). Pie charts show proportions of genetic types identified in each of the upper-, mid- and lower-shore samples. Numbers in brackets are the number of individuals genetically characterised. Lower-shore samples were taken at extreme low tide within four days of the low spring tide event. Upper-shore samples were collected from the marine sediment below the transition from sediment to grass. Mid-shore samples were taken approximately midway between the two, but using the mid-shore indicator seaweed, *Fucus vesiculosus*, as a guide.

Tables

Table 1. Description of sampling locations and the *Ammonia* genetic types identified.

Table 2. *Ammonia* SSU sequences used for phylogenetic analyses (Fig. 3) including sequences from this study and those previously deposited in GenBank. References are either where the sequences were first published or direct submissions to GenBank (DS). Accession numbers are shown with previously published sequences in italic and new ones (this study) in bold.

Table 3. Test characteristics measured or assessed from the umbilical and spiral SEM images of the *Ammonia* specimens. These measured morphological characteristics have been derived from Hayward et al. (2004) with some minor modifications. The qualitative five-point assessment utilised in this study includes: 1- None, 2- Very weak, 3- Weak, 4- Medium, and 5- Strong. The three-point scale utilised here includes: 1- Absent, 2- Moderately developed, 3- Strongly developed. Chamber N is equivalent to the final chamber, whilst N1 is the penultimate chamber etc.

Table 4. Conversion of SSU genetic types (S) from this study into the established T-type nomenclature originally based on the LSU (Holzmann and Pawlowski 2000; Hayward et al., 2004).

Table 5. Confusion matrix of the number of *Ammonia* specimens correctly and incorrectly classified into each genetic type in the Discriminant Function Analysis and cross validation procedure. Percentage of correctly classified individuals is also reported for each genetic type. T3V was not included in the DFA due to the small number of images available for analysis.

Table 6. Description of the biogeographical range, habitat and co-occurrence of the seven genetic types and subtypes identified in this study. The biogeographical ranges described include specimens whose sequences have been previously deposited in GenBank by others (Tables S1 and S5), and are as shown on maps Figs. 7 and 8. Biogeographic provinces are based on the OSPAR Maritime Areas (Dinter, 2001). Habitat descriptions and co-occurrences are based on this study and Saad, and Wade (2016).

Table 7. Number of specimens genetically characterised from each of the 22 sampling locations.

Supplementary figures

Fig. S1. Molecular phylogeny of *Ammonia* based on partial SSU sequences inferred using the ML method with the HKY+Γ model. The tree is unrooted and bootstrap values (1000 replicates) are indicated at the nodes.

Fig. S2. Molecular phylogeny of *Ammonia* based on partial SSU sequences inferred using the ML method with the GTR+Γ model. The tree is unrooted and bootstrap values (1000 replicates) are indicated at the nodes.

Fig. S3. Molecular phylogeny of *Ammonia* based on partial SSU sequences inferred using the BA method with the mixed model. The tree is unrooted and posterior probabilities are indicated at the nodes.

Supplementary tables

Table S1. *Ammonia* partial SSU sequences retrieved from the GenBank database (April 2015) used in the SSU alignment. References are either the articles where the sequences were first published or direct submissions (DS).

Table S2. The range of measurements of each morphological test characteristic for each genetic type. The qualitative five-point assessment utilised in this study (Table 3) includes: 1- None, 2- Very weak, 3- Weak, 4- Medium, and 5- Strong. The three-point scale utilised includes: 1- Absent, 2- Moderately developed, 3- Strongly developed.

Table S3. Number of *Ammonia* specimens genetically characterised by sequencing or screening and new SSU sequences submitted to GenBank (this study). SSU sequences already published in GenBank for each genetic type (July 2018) are also shown. Genetic types in bold are those represented in NE Atlantic margins.

Table S4: Link between SSU and LSU genetic types sequenced in the same individuals with GenBank accession numbers corresponding to each gene. Accession numbers in italics are previously published, those in bold are this study.

Table S5. *Ammonia* partial LSU sequences retrieved from the GenBank database (August 2015) with additional sequences from Saad and Wade (2016). References are either the articles where the sequences were first published or direct submissions (DS).

Supplementary information

Supplementary Data 1. Complete set of morphometric measurements for each *Ammonia* specimen morphometrically analysed.

Supplementary Data 2. Alignment of LSU sequences showing variability between genetic subtypes T2A and T2B, and T3S and T3V.

Supplementary Data 3. Alignment of SSU sequences showing minor variation between genetic subtypes T3S and T3V.

Table 1. Description of sampling locations and the *Ammonia* genetic types identified.

Location number (see map)	Location name	Multiple sampling site IDs	Co-ordinates	Site description	Genetic types identified (n=number genotyped)
1	Shetland (SH)		60^{o} 14' 31.20"N 01^{o} 22' 40.68"W	Subtidal sediment 12 m	T3S (n=12)
2	Cromarty (CR)		57° 40′ 45.59″N 04° 02′ 28.12″W	Intertidal sediment	T2A (n=1)
3	North Uist (NU)	Bagh a Chaise, Sound of Harris IT5SW	57° 38' 47.81"N 07° 04' 42.29"W	Intertidal seaweed	T3S (n=13)
		LPSW21	57° 37' 18.72"N 07° 09' 02.80"W	Seaweeds	T3S (n=3)
		LM1B	57° 36' 17.75"N 07° 09' 43.50"W	Seaweeds	T3S (n=14)
4	Loch Sunart (SU)		56° 39′ 56.80″N 05° 52′ 02.10″W	Subtidal sediment 30.6m	T1 (n=1) T3S (n=2) T15 (n=3)
5	Dunstaffnage (DF)		56°27′06.1″N 05°27′27.9″W	Subtidal sediment 31.6m	T1 (n=1) T3S (n=11) T15 (n=8)
6	Anholt, Kattegat (BA)		56° 26' 02.88"N 11° 50' 02.58"E	Sediment, 12-30m. Salinity 18-32	T3S (n=1) T15 (n=1)
7	Hanö Bay, Baltic (BA)		55° 38' 00.00"N 14° 50' 00.00"E	Sediment, 15-65m. Salinity 7-13	T6 (n=18)
8	Torry Bay (TB)		56°03' 28.3"N 03°35' 02.5"W	Intertidal estuarine soft muddy sediment	T6 (n=8)
9	Cramond (Cd)		55° 58' 54.2"N 03° 17' 56.5"W	Intertidal estuarine muddy sediment	T6 (n=52)
10	Loch na Cille (LK)		55° 57' 36.00"N 05° 41' 24.00"W	Intertidal muddy sediment	T2A (n=13) T3S (n=8)
11	Whiterock (WR)		54° 29' 05.42"N 05° 39' 12.58"W	Intertidal muddy sediment	T2A (n=18)
12	Den Oever (F)		**52°56'24.8"N 05°01'30.6"E**	Brackish water with local freshwater discharge. Intertidal sediment	T6 (n=1)
13	Norfolk (NF)		52° 49' 02.41"N 00°21' 46.16"E	Intertidal sediment	T6 (n=30) T2A (n=1)
14	Laugharne Castle (LC)		51° 46' 12.00"N 04° 27' 00.00"W	Intertidal estuarine sediment	T6 (n=2)
15	Grevelingen (Gv)		51° 44' 50.04"N 03° 53' 24.06"E	Lake with stratified water, saline/brackish, 34m	T6 (n=2)
16	Cork (CK)		51° 38' 29.40"N 08° 45' 44.50"W	Estuarine intertidal muddy sediment	T1 (n=2) T2B (n=28)
17	Cardiff (CF)		**51°29' 25.40" N 03° 07' 19.50"W**	Intertidal sediment	T6 (n=20)
18	Dartmouth (DM)	Upper shore	50° 21' 04.84"N 03° 34' 11.33"W	Intertidal estuarine very soft muddy sediment	T2A (n=6)
		Mid shore	50° 21' 04.84"N 03° 34' 11.33"W	Intertidal estuarine very soft muddy sediment	T1 (n=2) T2A (n=12) T3S (n=1)

		Lower shore	50° 21’ 04.84”N 03° 34’ 11.33”W	Intertidal estuarine very soft muddy sediment	T1 (n=2) T2A (n=49) T3S (n=14)
19	Ile d’Yeu (Ye)		46°43′ 12.35″N 02° 20′ 13″ W	Intertidal sediment with seaweeds	T3V (n=10)
20	Baie de l’Aiguillon (Ai)		46° 15' 17.00"N 01° 08'27.00"W	Intertidal sediment	T6 (n=2)
21	Rhône prodelta (Rh/F)	BEHEMOTH, station 15	43°17.055’ N 04°45.148’ E	Subtidal sediment, 60m	T15 (n=1)
		CHACCRA Bent 1, station I	43°15.810 N 04°52.916 E	Subtidal sediment, 88m	T3S (n=1)
		Riotinto, station L	43°18.58 N 04°52.84 E	Subtidal sediment, 55m	T3S (n=1) T15 (n=1)
22	Portuguese margin (Po)	Po11-6/1	41° 07’ 48.3”N 09° 05’ 05.3”W	Organic matter, 110m	T3S (n=1) T15 (n=1)
		Po11-17/2	38° 56’ 00.8”N 09° 28’ 32.4”W	Sand, 48m	T3S (n=1)
		Po11-17/3	41° 09’ 01.2”N 08° 52’ 00.9”W	Sand, 50m	T3S (n=4)
		Po11-18/5	39° 01’ 53.0”N 09° 40’ 26.5”W	Mud, 116m	T15 (n=1)

Table 2. *Ammonia* SSU sequences used for phylogenetic analyses (Fig. 3) including sequences from this study and those previously deposited in GenBank. References are either where the sequences were first published or direct submissions to GenBank (DS). Accession numbers are shown with previously published sequences in italic and new ones (this study) in bold.

Genetic Type	Accession Number	DNA isolate	Location name	Location number, Fig. 1 and Table 1	Depth	Reference
S1 (T6)	**MH124850**	NF92	Norfolk, UK	13	intertidal	This study
S1 (T6)	**MH124874**	CF02E	Cardiff, UK	17	intertidal	This study
S1 (T6)	**MH124875**	CF03A	Cardiff, UK	17	intertidal	This study
S1 (T6)	**MH124903**	Ai11	Baie de l'Aiguillon, France	20	intertidal	This study
S1 (T6)	*AF190874*		Crildumersiel, Germany		intertidal	Langer & Leppig 2000
S1 (T6)	*AF190879*		Crildumersiel, Germany		intertidal	Langer & Leppig 2000
S1 (T6)	*AF533835*		Amrum, Germany		intertidal	Ertan et al. 2004
S1 (T6)	*FR839692*		East China			Pawlowski & Holzmann 2011 (DS)
S1 (T6)	*GQ853573*		Kiel Fjord, Germany		10-20m	Schweizer et al. 2011a
S2 (T2A)	**MH124941**	WR39D	Whiterock, UK	11	intertidal	This study
S2 (T2A)	**MH124944**	WR41C	Whiterock, UK	11	intertidal	This study
S2 (T2A)	**MH124915**	DM42C	Dartmouth, UK	18	intertidal	This study
S2 (T2A)	**MH124918**	DM43	Dartmouth, UK	18	intertidal	This study
S2 (T2A)	*FR754385*		Camargue, France			Pawlowski & Holzmann 2010 (DS)
S2 (T2A)	*FR754387*		Golf du Morbihan, France			Pawlowski & Holzmann 2010 (DS)
S2 (T2A)	*HE598565*		Dovey Estuary, UK			Pawlowski & Holzmann 2011 (DS)
S3 (T2B)	**MH124969**	CK05A	Cork, Ireland	16	intertidal	This study
S3 (T2B)	**MH124970**	CK05D	Cork, Ireland	16	intertidal	This study
S3 (T2B)	**MH124973**	CK28B	Cork, Ireland	16	intertidal	This study
S3	**MH124974**	CK28C	Cork, Ireland	16	intertidal	This study

(T2B)						
S3 (T2B)	*AY210767*		Ile d'Yeu, France		intertidal	Ertan et al. 2004
S3 (T2B)	*AY359128*		Ile d'Yeu, France		intertidal	Ertan et al. 2004
S3 (T2B)	*AY359129*		Ile d'Yeu, France		intertidal	Ertan et al. 2004
S3 (T2B)	*FM999843*		Bay of Biscay, France			Grimm et al. 2009 (DS)
S3 (T2B)	*HE598564*		Venice, Italy		?	Pawlowski & Holzmann 2011 (DS)
S3 (T2B)	*X86094*		Camargue, France			Pawlowski et al.1996*
S3 (T2B)	*Z69616*		Camargue, France		?	Pawlowski et al. 1997
S4 (T1)	**MH125002**	CK20	Cork, Ireland	16	intertidal	This study
S4 (T1)	**MH125006**	CK54	Cork, Ireland	16	intertidal	This study
S4 (T1)	*FR754382*		Playa Bailen, Cuba			Pawlowski & Holzmann 2010 (DS)
S4 (T1)	*HE598562*		Waitemata Harbour, New Zealand			Pawlowski & Holzmann 2011 (DS)
S4 (T1)	*HE598563*		Playa Bailen, Cuba			Pawlowski & Holzmann 2011 (DS)
S4 (T1)	*Z69617*		Camargue, France		?	Pawlowski et al. 1997
S4 (T1)	*AY465834*		Ile d'Yeu, France		intertidal	Ertan et al. 2004
S5a (T3S)	**MH125016**	DF18B	Dunstaffnage, UK	5	subtidal	This study
S5a (T3S)	**MH125032**	DM10D	Dartmouth, UK	18	intertidal	This study
S5a (T3S)	**MH125074**	F432	Rhône Prodelta, France	21	88m	This study
S5a (T3S)	**MH125065**	Po203C	Portuguese margin	22	110m	This study
S5a (T3S)	**MH125070**	Po220	Portuguese margin	22	50m	This study
S5a (T3S)	*FR839705*		Tjärnö, Sweden			Pawlowski & Holzmann 2011 (DS)
S5a (T3S)	*FR839708*		Tjärnö, Sweden			Pawlowski & Holzmann 2011 (DS)
S5b (T3V)	**MH125076**	Ye32	Ile d'Yeu, France	19	intertidal	This study
S5b (T3V)	**MH125080**	Ye60A	Ile d'Yeu, France	19	intertidal	This study
S5b (T3V)	**MH125094**	Ye75A	Ile d'Yeu, France	19	intertidal	This study
S5b (T3V)	**MH125078**	Ye125	Ile d'Yeu, France	19	intertidal	This study
S5b (T3V)	*EF534072*		?		?	Schweizer et al. 2008

S6 (T15)	**MH125130**	SU134	Loch Sunart	4	subtidal	This study
S6 (T15)	**MH125114**	DF94	Dunstaffnage	5	subtidal	This study
S6 (T15)	**MH125149**	F187H	Rhône Prodelta	21	60m	This study
S6 (T15)	**MH125132**	Po202A	Portuguese margin	22	110m	This study
S6 (T15)	*HM448841*		Rhône Prodelta, France		60m	Schweizer et al. 2011b
T4	*FR839697*		Hamana Lake, Japan			Pawlowski & Holzmann 2011 (DS)
T4	*FR839698*		Hamana Lake, Japan			Pawlowski & Holzmann 2011 (DS)
T4	*FR839699*		Hamana Lake, Japan			Pawlowski & Holzmann 2011 (DS)
T4	*FR839700*		Hamana Lake, Japan			Pawlowski & Holzmann 2011 (DS)
T5	*FR839689*		Pollen Island, New Zealand			Pawlowski & Holzmann 2011 (DS)
T5	*FR839690*		Pollen Island, New Zealand			Pawlowski & Holzmann 2011 (DS)
T7	*FR839702*		Sapelo Island, USA			Pawlowski & Holzmann 2011 (DS)
T7	*FR839703*		Sapelo Island, USA			Pawlowski & Holzmann 2011 (DS)
T8	*FR839751*		Taba, Israel			Pawlowski & Holzmann 2011 (DS)
T9	*FR839747*		Long Island, USA			Pawlowski & Holzmann 2011 (DS)
T9	*FR839748*		Long Island, USA			Pawlowski & Holzmann 2011 (DS)
T10	*FR839693*		Grays Harbour, USA			Pawlowski & Holzmann 2011 (DS)
T10	*FR839694*		Grays Harbour, USA			Pawlowski & Holzmann 2011 (DS)
T10	*FR839695*		Grays Harbour, USA			Pawlowski & Holzmann 2011 (DS)
T10	*FR839696*		Grays Harbour, USA			Pawlowski & Holzmann 2011 (DS)
T11	*FR839709*		Playa Bailen, Cuba			Pawlowski & Holzmann 2011 (DS)
T12	*FR839712*		Tieti Beach, New Caledonia			Pawlowski & Holzmann 2011 (DS)
T12	*FR839713*		Tieti Beach, New Caledonia			Pawlowski & Holzmann 2011 (DS)
T13	*FR839710*		Noumea, New Caledonia			Pawlowski & Holzmann 2011 (DS)
T13	*FR839711*		Noumea, New Caledonia			Pawlowski & Holzmann 2011 (DS)
T14	*GQ853567*	475	Lizard Island, Australia			Schweizer et al. 2011a
T14	*GQ853568*	476	Lizard Island, Australia			Schweizer et al. 2011a

Table 3. Test characteristics measured or assessed from the umbilical and spiral SEM images of the *Ammonia* specimens. These measured morphological characteristics have been derived from Hayward et al. (2004) with some minor modifications. The qualitative five-point assessment utilised in this study includes: 1- None, 2- Very weak, 3- Weak, 4- Medium, and 5- Strong. The three-point scale utilised here includes: 1- Absent, 2- Moderately developed, 3- Strongly developed. Chamber N is equivalent to the final chamber, whilst N1 is the penultimate chamber etc.

Type of character	**Variable Number**	**Corresponding variable number in Hayward et al (2004)**	**Morphological feature name**	**Method of measurement**	**Unit/ Category/ Type**
Umbilical View					
Quantitative	**1**	7	Relative diameter of the umbilical area	Largest diameter of umbilicus between the ends of the folia/ maximum test diameter	Ratio
Quantitative	**2**	10	Relative maximum boss diameter	Maximum diameter of the largest umbilical boss (if present)/ maximum diameter	Ratio
Quantitative	**3**	11	Total number of umbilical bosses	Number of umbilical bosses (if present)	Count
Quantitative	**4**	n/a	Radial curvature of suture N1	Curvature of suture between chambers N1 and N2. This feature was calculated using the arc tool in Image Pro Express	Angle
Quantitative	**5**	n/a	Mean pore diameter	Mean pore diameter of the ten pores nearest the junction between chamber N1 and chamber N2	Micrometres

Quantitative	**6**	n/a	Total number of chambers visible	Total number of chambers visible/ maximum test diameter	Ratio
Quantitative	**7**	n/a	Relative width of radial suture	Maximum width of suture nearest to the umbilical area/ maximum width of suture at the test periphery	Ratio
Categorical	**8**	13	Degree of development of thickened calcite on folia	Development of thickened calcite on chambers N-N3	1 to 3 scale
Categorical	**9**	16	Degree of blunt ragged folia	Blunt ragged folia on chambers N- N3	1 to 5 Scale
Categorical	**10**	20	Development of beading on the folia	Folia cut into flat beads by grooves on chambers N-N3	Presence/ absence
Categorical	**11**	18	Development of beading along the radial sutures	Development of strong beads along edge of radial sutures on chambers N-N3	1 to 5 scale
Categorical	**12**	14	Degree of ornamentation on folia	Coverage of folia by small pustules on chambers N-N3	1 to 5 scale
Categorical	**13**	19	Development of grooved notches	Development of grooved notches along radial edge of sutures	1 to 5 scale
Categorical	**14**	n/a	Development of small pustules on radial edge of sutures	Development of small pustules along the radial edge of sutures in chamber N-N3	1 to 5 scale
Spiral view					
Quantitative	**15**	22	Number of chambers in the first whorl	Total number of chambers in the first whorl	Count
Quantitative	**16**	26	Relative chamber proportions	Maximum length (parallel to the periphery) of chamber N1/ maximum width (perpendicular to periphery) of the chamber	Ratio
Quantitative	**17**	Modified variable 27	Test roundness	As calculated from the outline of the entire shape utilising the Image outline analysis tool in Image J software (Roberts, 2016)	0 to 1
Quantitative	**18**	29	Angle between radial and spiral sutures	Angle between radial and spiral sutures in Chamber N1	Angle
Quantitative	**19**	28	Relative length of fissure	Length of fissure along the spiral suture (when present)/ maximum test diameter	Ratio
Quantitative	**20**	36	Mean pore diameter	Mean pore diameter of the 10 nearest pores to the junction between chamber N1 and chamber N2	Micrometres
Quantitative	**21**	37	Pore density	Pore density was calculated from total number of pores/ 100 sq µm	Count
Quantitative	**22**	21	Proloculus diameter	Maximum diameter of the proloculus	Micrometres
Categorical	**23**	30	Development of radial suture furrows	Development of furrows along radial sutures (when present)	1 to 5 scale
Categorical	**24**	33	Development of thickened calcite	Development of raised thickened calcite over central spiral area	1 to5 scale

Categorical	**25**	n/a	Development of secondary dorsal openings	Development of discrete non-continuous secondary dorsal openings	Presence (1) / Absence (2)

Table 4. Conversion of SSU genetic types (S) from this study into the established T-type nomenclature originally based on the LSU (Holzmann and Pawlowski 2000; Hayward et al., 2004).

SSU genetic type (this study)	LSU genetic type (Hayward et al., 2014)
S1	T6
S2	T2A
S3	T2B
S4	T1
S5a	T3S
S5b	T3V
S6	T15

Table 5. Confusion matrix of the number of *Ammonia* specimens correctly and incorrectly classified into each genetic type in the Discriminant Function Analysis and cross validation procedure. Percentage of correctly classified individuals is also reported for each genetic type. T3V was not included in the DFA due to the small number of images available for analysis.

Discriminant Function Analysis (DFA)							
Number of specimens	**T1**	**T2A**	**T2B**	**T3S**	**T6**	**T15**	**Percentage correctly classified**
T1	4	0	0	0	0	0	100
T2A	0	70	0	0	0	0	100
T2B	0	2	14	0	0	0	87.5
T3S	0	0	0	8	0	0	100
T6	0	1	0	0	49	0	98
T15	0	0	0	0	0	8	100
Cross Validation Procedure							
	T1	**T2A**	**T2B**	**T3S**	**T6**	**T15**	
T1	1	0	0	0	3	0	25
T2A	0	70	0	0	0	0	100
T2B	0	4	12	0	0	0	75
T3S	0	0	0	8	0	0	100
T6	1	2	1	0	46	0	92
T15	1	2	1	0	0	4	50

Table 6. Description of the biogeographical range, habitat and co-occurrence of the seven genetic types and subtypes identified in this study. The biogeographical ranges described include specimens whose sequences have been previously deposited in Genbank by others (Tables S1 and S5), and are as shown on maps Figs. 7 and 8. Biogeographic zones are based on the OSPAR Maritime Areas (Dinter, 2001). Habitat descriptions and co-occurrences are based on this study and Saad and Wade (2016).

e	Map	Biogeographical range within the study area	Habitat preferences	Obse occu
	Fig. 7a	Rare in our data set, but broadly reported by others. Range extends from the Skagerrak subprovince through to the Lusitanean-Boreal province. Also reported in the Mediterranean Sea.	Intertidal mudflats including estuarine systems, and high salt marsh. Soft deep muddy sediments and muddy sand. Rarely subtidal (only observed two specimens, 30 m).	T2A, T2E
	Fig. 7b	Distribution ranges from the Boreal province to the Lusitanean-Boreal province with samples also identified in the Mediterranean Sea. In the Boreal province, T2 has only been identified on the UK coast, and to date has not been reported on the coast of mainland Europe including Scandinavia.	Intertidal mudflats including estuarine systems, and high salt marsh. Found at extreme high through to low shore, able to tolerate reduced tidal coverage. Soft deep muddy sediments and muddy sand.	T1, T3S,
	Fig. 7c	A warmer water genetic type, rare in our sample set. Unusually, it is not reported in the Boreal province to date. It ranges from the Boreal-Lusitanean province to the Warm Lusitanean subprovince and is also present in the Mediterranean.	Intertidal mudflats in estuarine systems. Soft muddy sediments and hard muddy sand.	T1, T6
	Fig. 8a	The most northerly distributed genetic type in our data set, it ranges from the Shetland Islands in the Boreal Province and the Skagerrak subprovince, to the Cool-Lusitanean province. This genetic type is also identified in the Mediterranean Sea.	Abundant in both intertidal and subtidal muddy sediments and seaweeds. Rarely estuarine. Found from mid-intertidal shore to deepest sampled sediments of 116m.	T1, T2A,
	Fig. 8b	Very limited biogeographical range, identified only in the Lusitanean-Boreal province in the region of Vendée, on the French Atlantic coast.	Currently identified only on intertidal seaweeds at a single location.	None
	Fig. 7d	An extremely abundant genetic type throughout the Boreal province. Also identified in the Baltic Sea and the Boreal-Lusitanean province, extending into the Lusitanean-Boreal province. Not yet reported in the Mediterranean.	Predominantly brackish intertidal mudflats, particularly in estuarine environments but not exclusively. Low salt marsh environments. Soft deep muddy sediment through to hard muddy sand. Also found subtidally at low salinities (e.g. 7-13 in the Baltic Sea).	T2A, T2E
	Fig. 8c	Ranges from the Kattegat Sea in the Boreal Province to the Cool Lusitanean subprovince. Also identified in the Mediterranean Sea.	Fully marine subtidal species found in marine sediments.	T3S

Table 7. Number of specimens genetically characterised from each of the 22 locations

	Shetland (Sh)	**Cromarty (CR)**	**North Uist (NU)**	**Loch Sunart (SU)**	**Dunstaffnage (DF)**	**Anholt, Kattegat (BA)**	**Hanö Bay, Baltic (BA)**	**Torry Bay (TB)**	**Cramond (Cd)**	**Loch na Cille (LK)**	**White Rock (WR)**	**Den Oever (F)**	**Norfolk (NF)**	**Laugharne (LC)**	**Grevelingen (Gv)**	**Cork (CK)**	**Cardiff (CF)**	**Dartmouth (DM)**	**Ile d'Yeu (Ye)**	**Baie de l'Aiguillon (Ai)**	**Rhône prodelta (Rh/F)**	**Portuguese Margin**
Location number on Figure 1	**1**	**2**	**3**	**4**	**5**	**6**	**7**	**8**	**9**	**10**	**11**	**12**	**13**	**14**	**15**	**16**	**17**	**18**	**19**	**20**	**21**	**22**
Genetic type																						
T1 (S4)				1	1											2		4				
T2 A (S2)		1								14	18		1					67				
T2 B (S3)																25						
T3S (S5 a)	12		30	2	11	1				7								14			2	6
T3 V (S5 b)																			8			
T6 (S1)							18	8	52			1	30	2	2		20			2		
T15 (S6)				3	8	1															2	2
Total	12	1	30	6	20	2	18	8	52	21	18	1	31	2	2	27	20	86	8	2	4	8

Highlights

- Largest ever survey of *Ammonia* sp. in the Northeast Atlantic margins to aid taxonomic delineation
- All specimens are SEM imaged, SSU genotyped and morphometrically analysed
- Of seven genetic types and subtypes, four are partially cryptic, but can co-occur
- Genetic types have different biogeographies and ecologies, aiding identification
- Taxonomic assignment is currently possible for only three of the genetic types

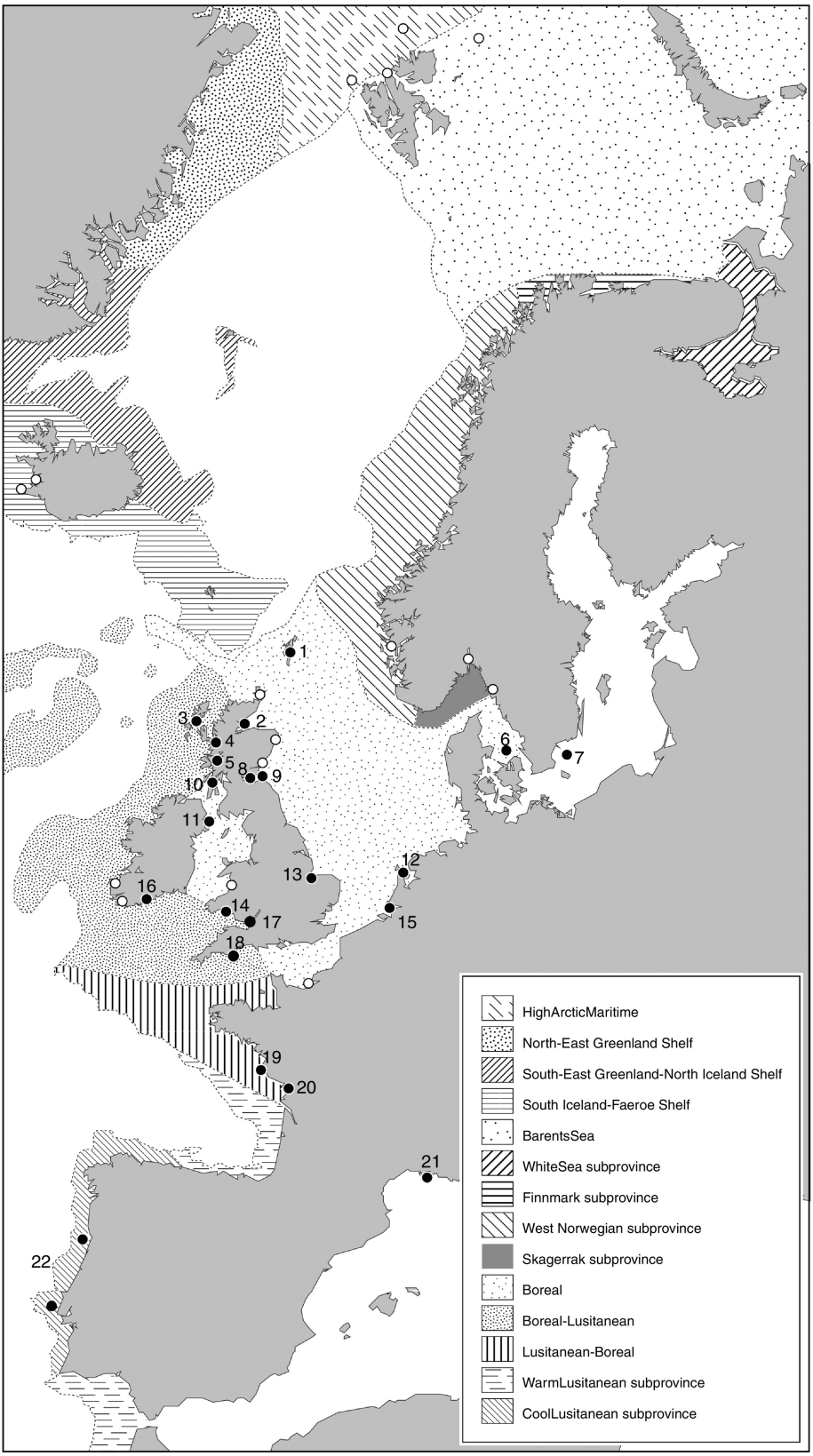

- Sample locations where Ammonia specimenswere successfully genotyped
- Sample locations where no Ammonia specimens werefound in this study.

Figure 1

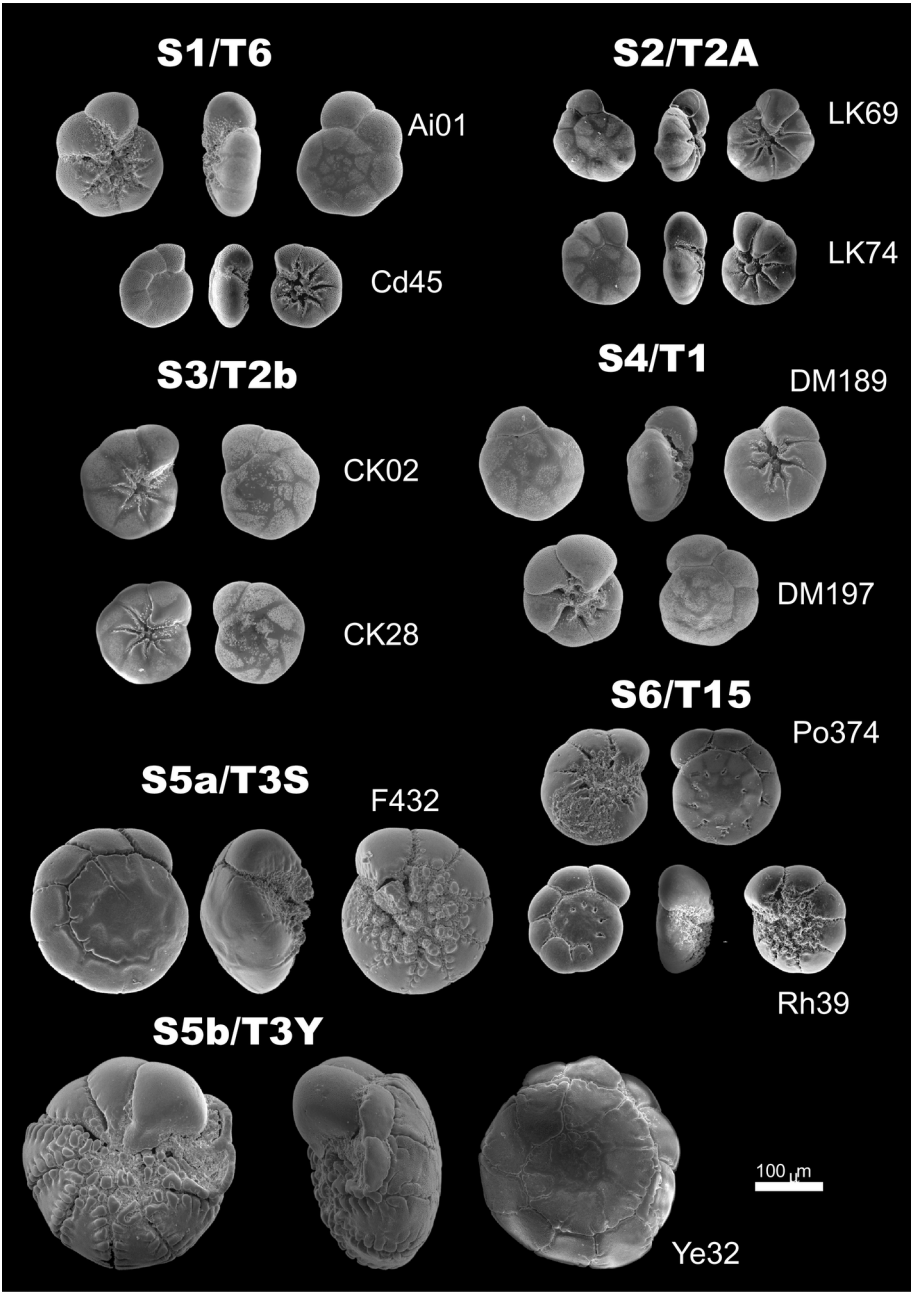
S1/T6
Ai01
Cd45
S2/T2A
LK69
LK74
S3/T2b
CK02
CK28
S4/T1
DM189
DM197
S6/T15
Po374
Rh39
S5a/T3S
F432
S5b/T3Y
Ye32
100 µm

Figure 2

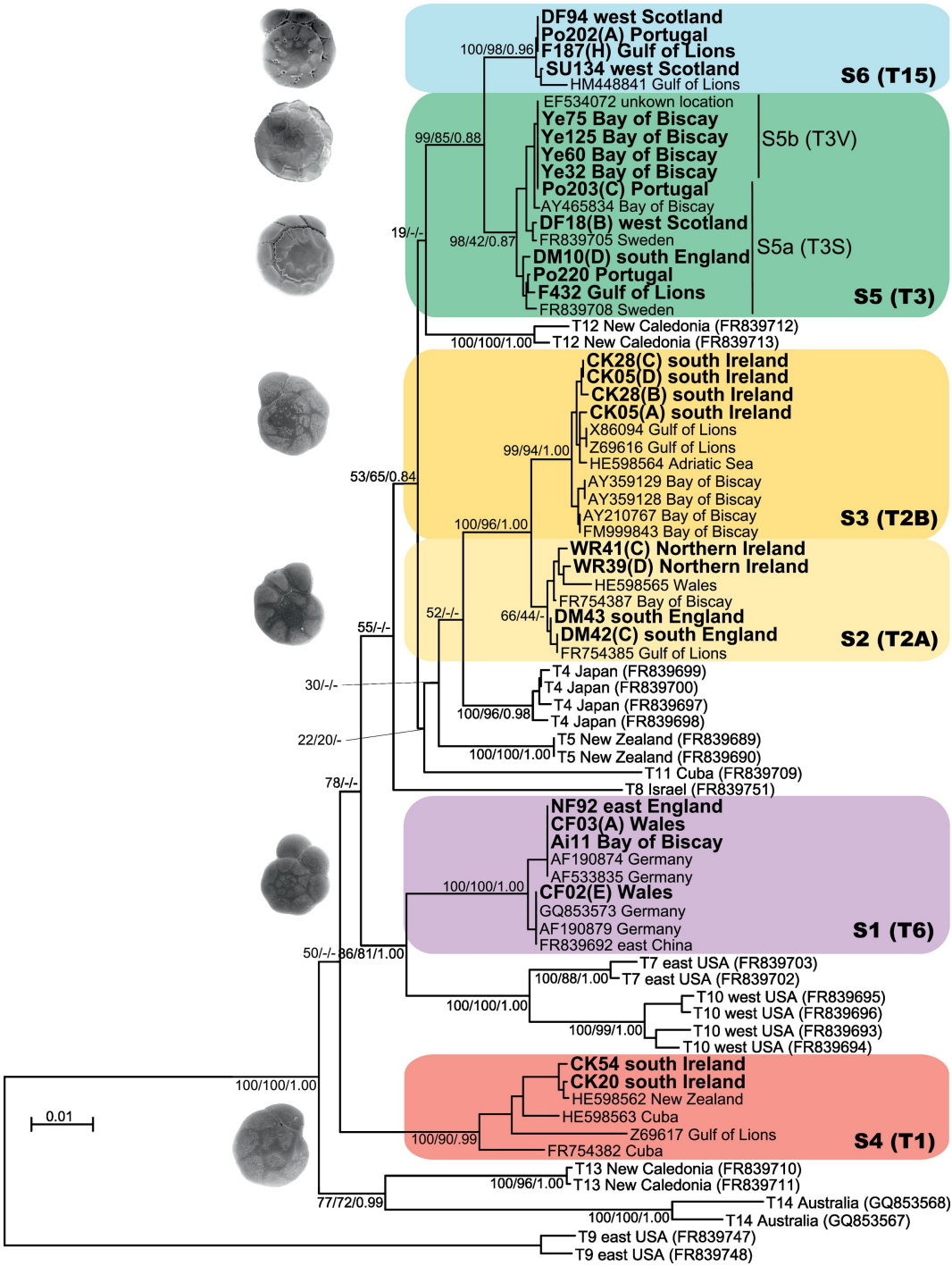
DF94 west Scotland
Po202(A) Portugal
F187(H) Gulf of Lions
SU134 west Scotland
HM448841 Gulf of Lions
S6 (T15)
100/98/0.96
EF534072 unkown location
Ye75 Bay of Biscay
Ye125 Bay of Biscay
Ye60 Bay of Biscay
Ye32 Bay of Biscay
Po203(C) Portugal
AY465834 Bay of Biscay
DF18(B) west Scotland
FR839705 Sweden
DM10(D) south England
Po220 Portugal
F432 Gulf of Lions
FR839708 Sweden
S5b (T3V)
S5a (T3S)
S5 (T3)
99/85/0.88
19/-/-
98/42/0.87
T12 New Caledonia (FR839712)
T12 New Caledonia (FR839713)
100/100/1.00
CK28(C) south Ireland
CK05(D) south Ireland
CK28(B) south Ireland
CK05(A) south Ireland
X86094 Gulf of Lions
Z69616 Gulf of Lions
HE598564 Adriatic Sea
AY359129 Bay of Biscay
AY359128 Bay of Biscay
AY210767 Bay of Biscay
FM999843 Bay of Biscay
S3 (T2B)
99/94/1.00
53/65/0.84
100/96/1.00
WR41(C) Northern Ireland
WR39(D) Northern Ireland
HE598565 Wales
FR754387 Bay of Biscay
DM43 south England
DM42(C) south England
FR754385 Gulf of Lions
S2 (T2A)
52/-/-
66/44/-
55/-/-
30/-/-
T4 Japan (FR839699)
T4 Japan (FR839700)
T4 Japan (FR839697)
T4 Japan (FR839698)
100/96/0.98
22/20/-
T5 New Zealand (FR839689)
T5 New Zealand (FR839690)
100/100/1.00
T11 Cuba (FR839709)
T8 Israel (FR839751)
78/-/-
NF92 east England
CF03(A) Wales
Ai11 Bay of Biscay
AF190874 Germany
AF533835 Germany
CF02(E) Wales
GQ853573 Germany
AF190879 Germany
FR839692 east China
S1 (T6)
100/100/1.00
50/-/-
86/81/1.00
T7 east USA (FR839703)
T7 east USA (FR839702)
100/88/1.00
T10 west USA (FR839695)
T10 west USA (FR839696)
100/100/1.00
T10 west USA (FR839693)
T10 west USA (FR839694)
100/99/1.00
CK54 south Ireland
CK20 south Ireland
HE598562 New Zealand
HE598563 Cuba
Z69617 Gulf of Lions
FR754382 Cuba
S4 (T1)
100/90/.99
100/100/1.00
0.01
T13 New Caledonia (FR839710)
T13 New Caledonia (FR839711)
100/96/1.00
77/72/0.99
T14 Australia (GQ853568)
T14 Australia (GQ853567)
100/100/1.00
T9 east USA (FR839747)
T9 east USA (FR839748)

Figure 3

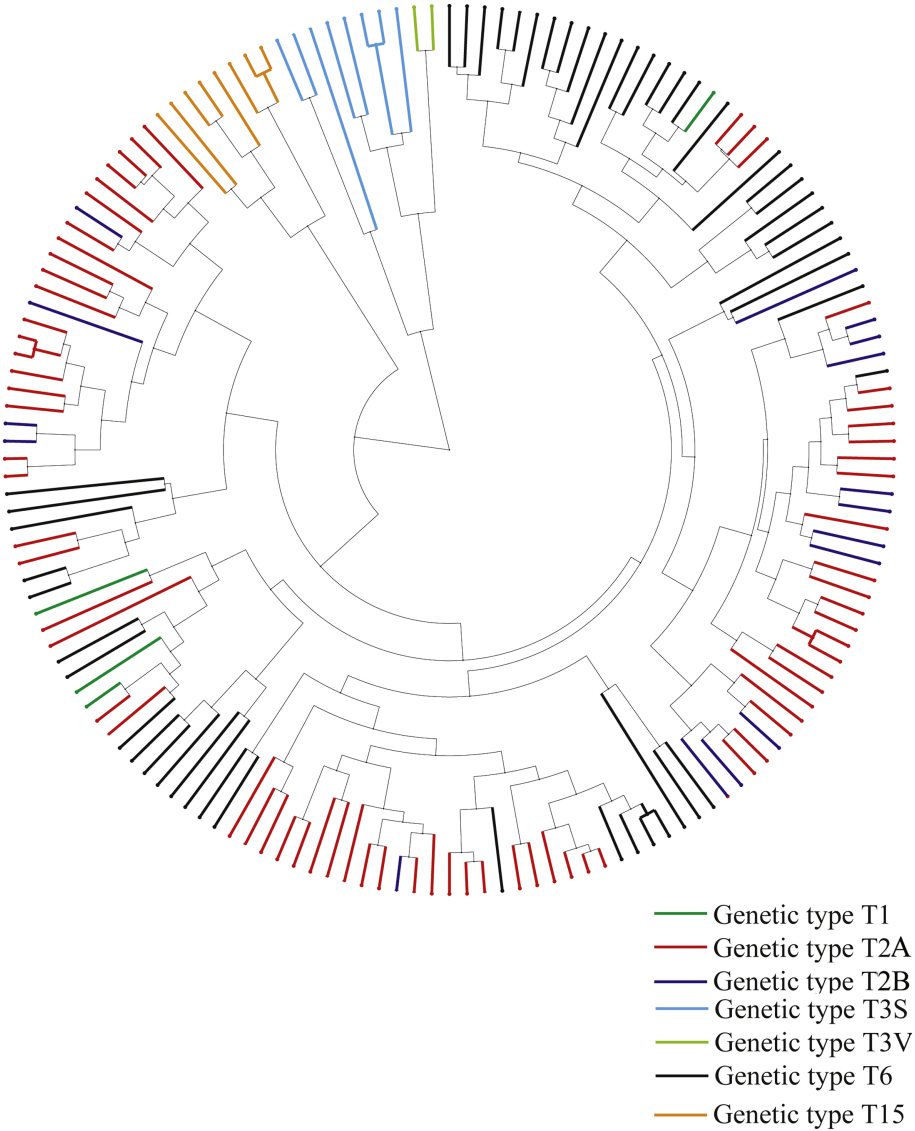
Genetic type T1
Genetic type T2A
Genetic type T2B
Genetic type T3S
Genetic type T3V
Genetic type T6
Genetic type T15

Figure 4

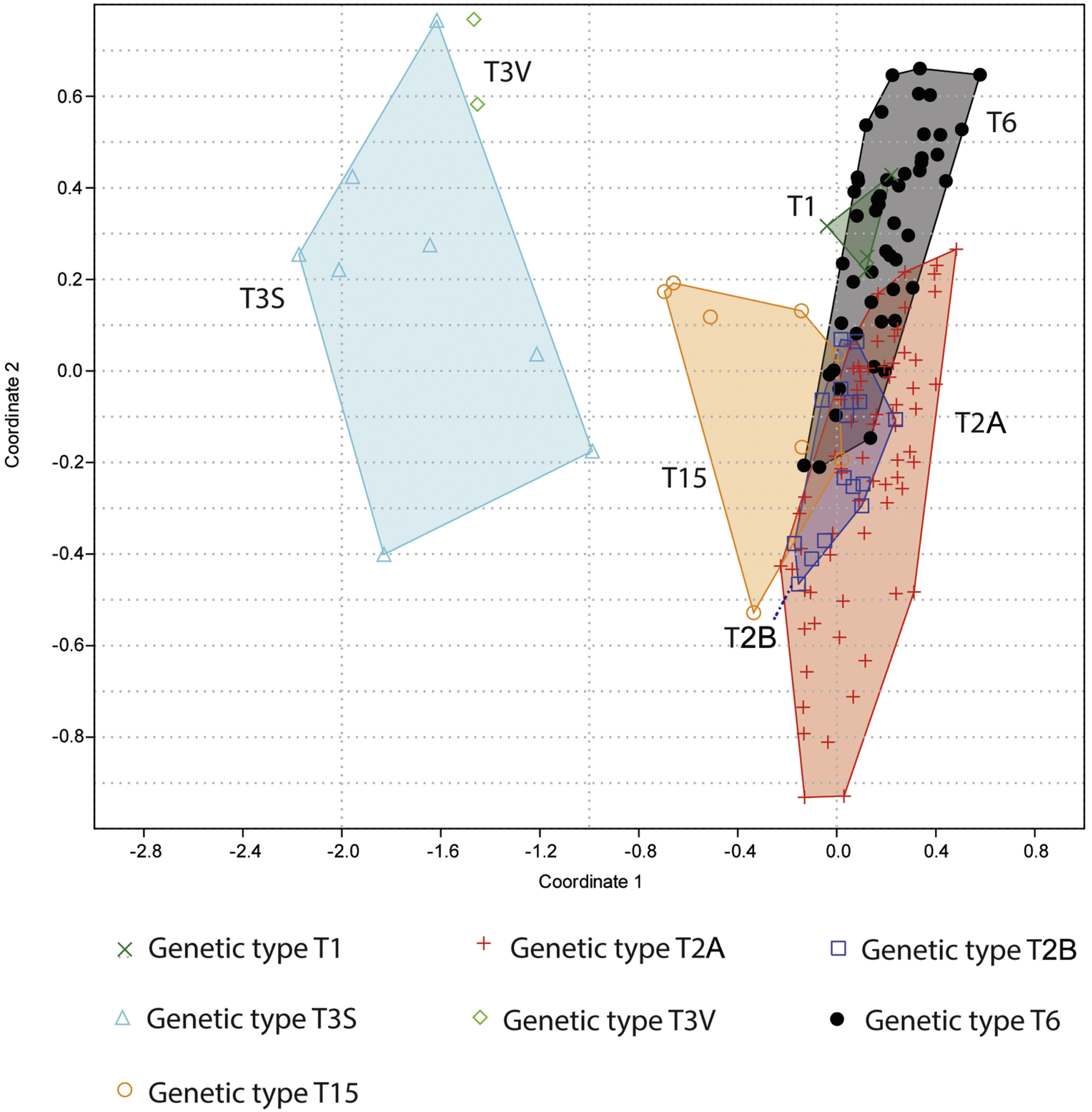
T3V
T6
T1
T3S
T15
T2A
T2B
0.6
0.4
0.2
0.0
-0.2
-0.4
-0.6
-0.8
Coordinate 2
-2.8
-2.4
-2.0
-1.6
-1.2
-0.8
-0.4
0.0
0.4
0.8
Coordinate 1
Genetic type T1
Genetic type T2A
Genetic type T2B
Genetic type T3S
Genetic type T3V
Genetic type T6
Genetic type T15

Figure 5

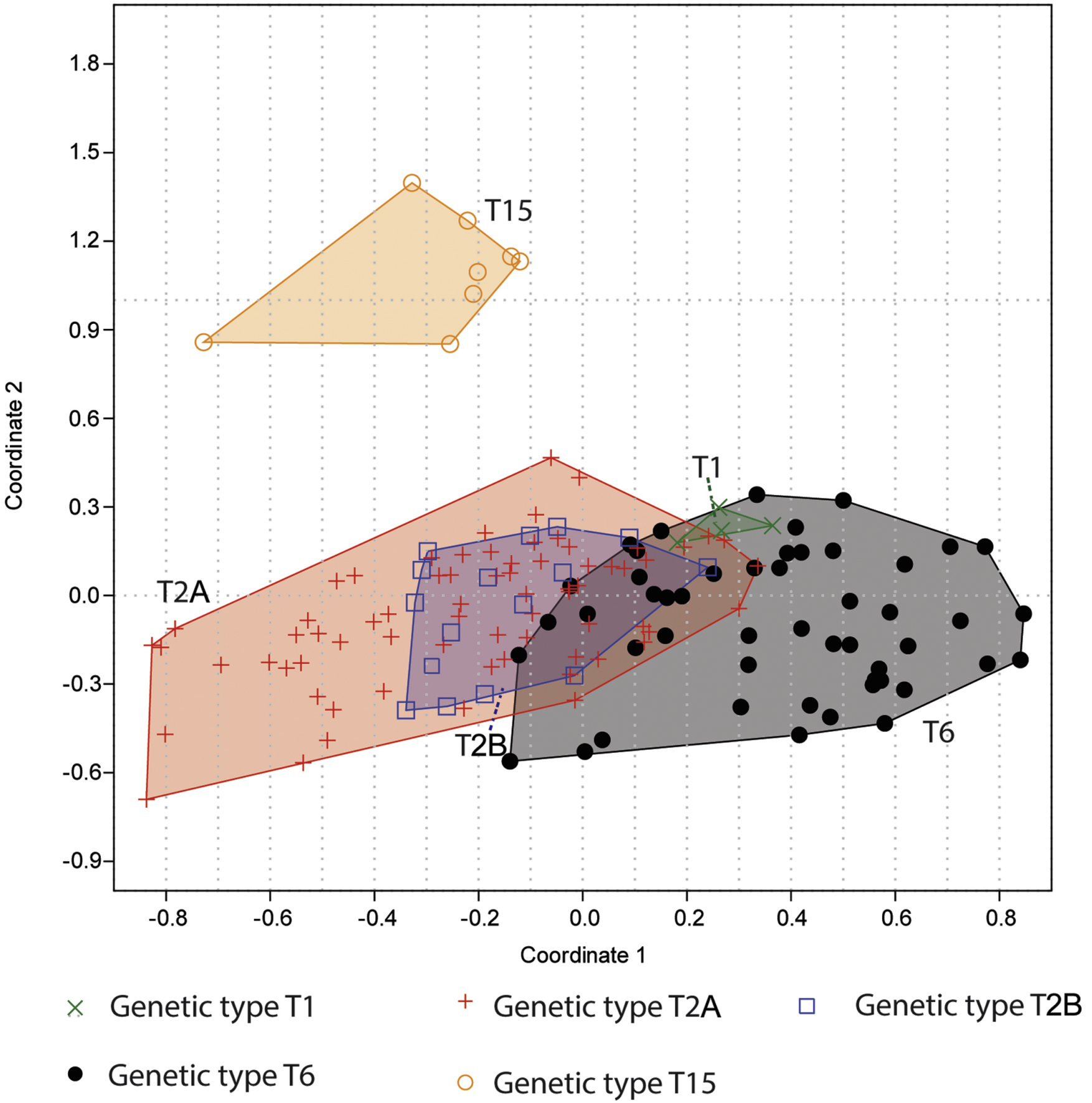
T15
T1
T2A
T2B
T6
Coordinate 1
Coordinate 2
1.8
1.5
1.2
0.9
0.6
0.3
0.0
-0.3
-0.6
-0.9
-0.8
-0.6
-0.4
-0.2
0.0
0.2
0.4
0.6
0.8
Genetic type T1
Genetic type T2A
Genetic type T2B
Genetic type T6
Genetic type T15

Figure 6

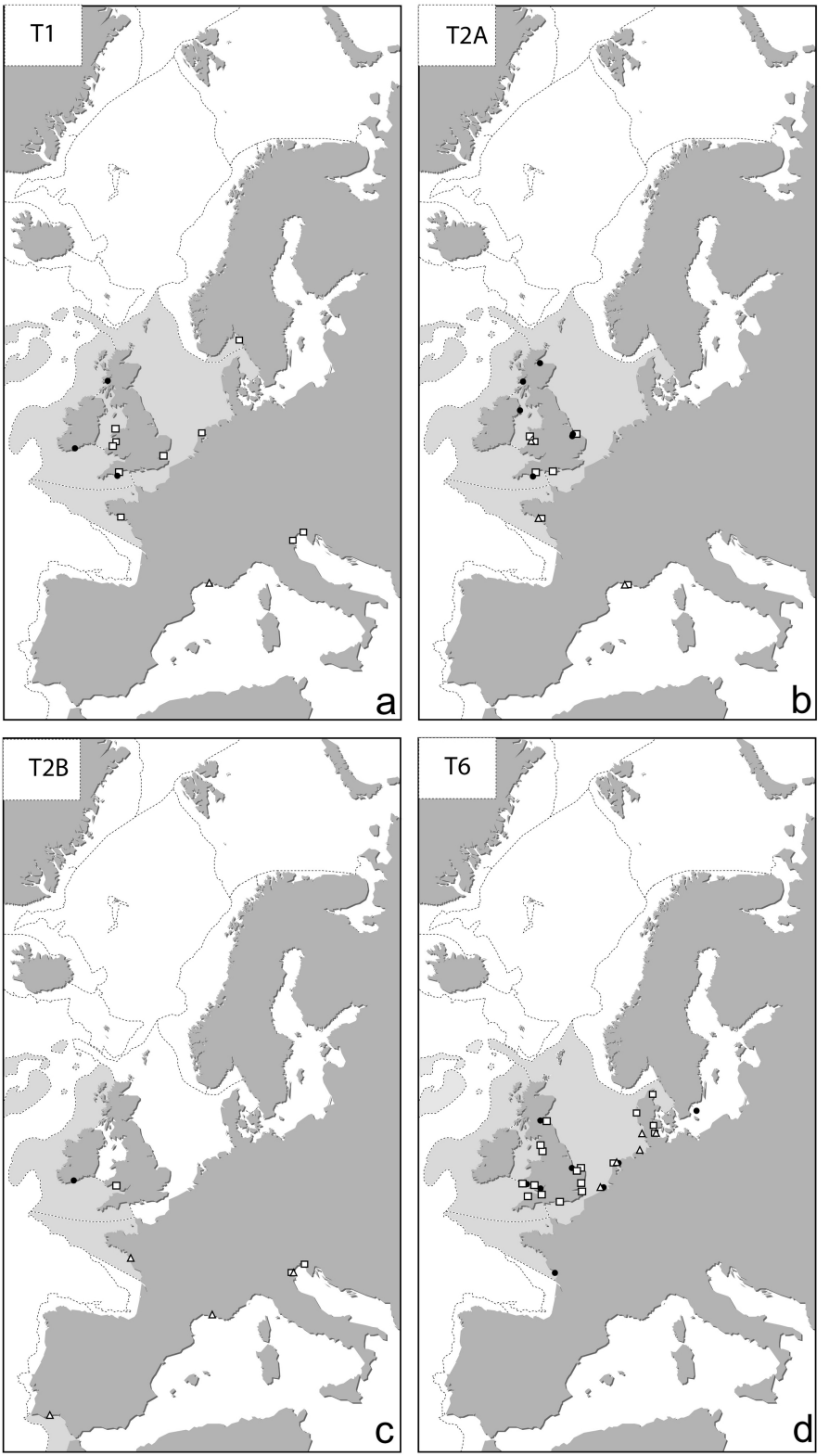
T1
a
T2A
b
T2B
c
T6
d
• Genetically identified in this study
△ Genbank sequence SSU
□ Genbank sequence LSU and RFLP

Figure 7

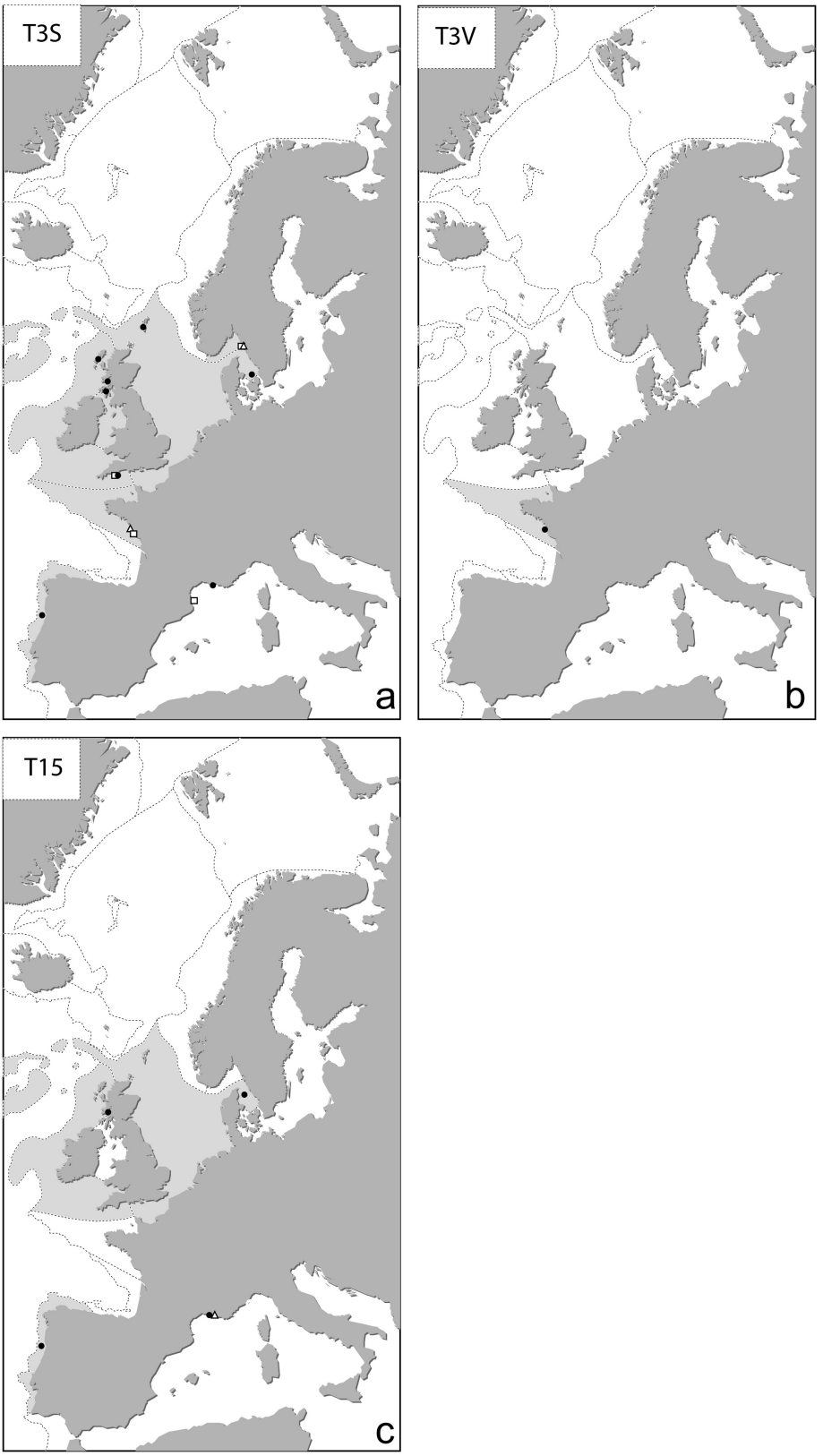
T3S
a
T3V
b
T15
c
Genetically identified in this study
Genbank sequence SSU
Genbank sequence LSU

Figure 8

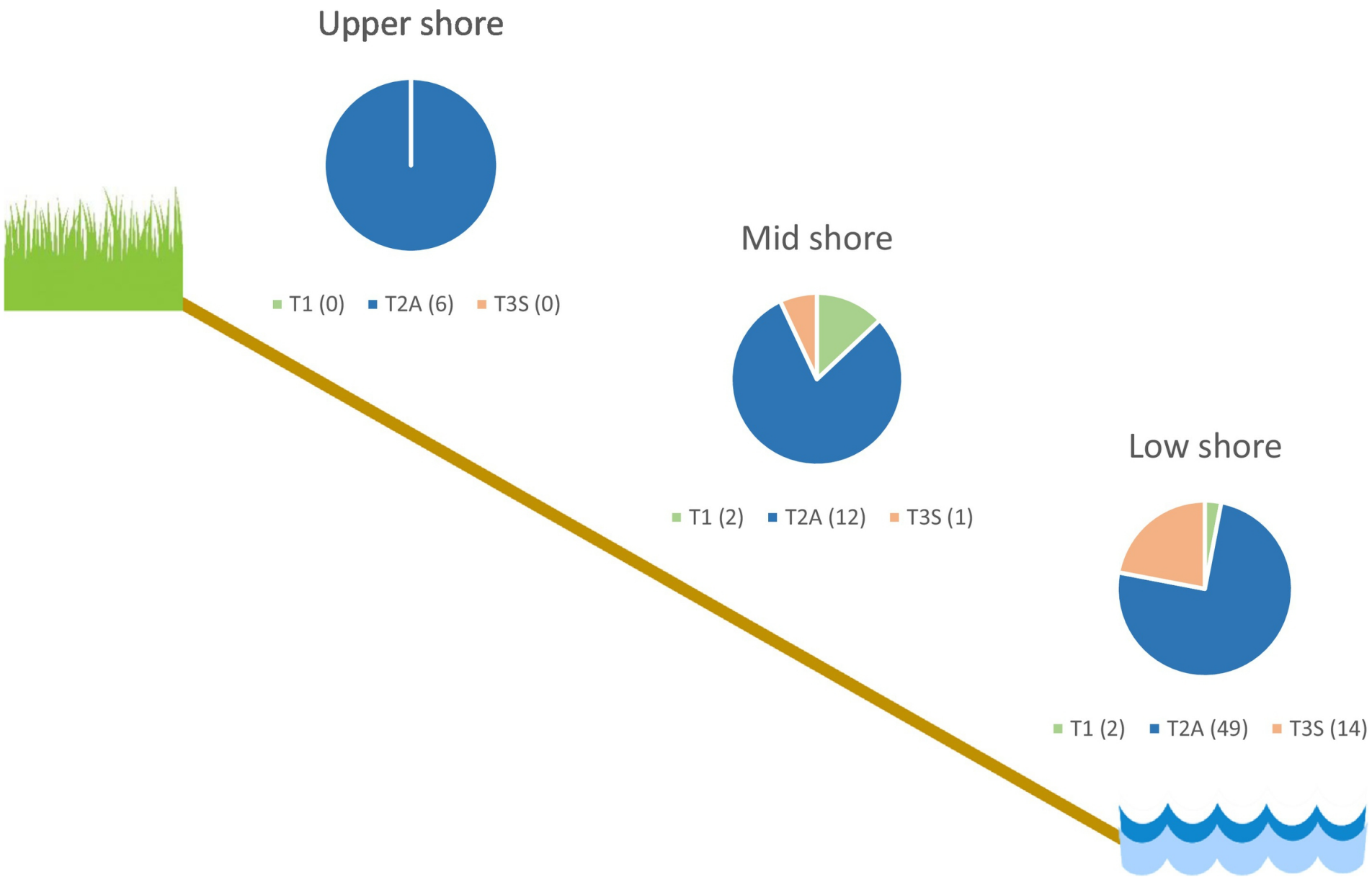
Upper shore
T1 (0)
T2A (6)
T3S (0)
Mid shore
T1 (2)
T2A (12)
T3S (1)
Low shore
T1 (2)
T2A (49)
T3S (14)

Figure 9